Configurations and conformations of glycosyl sulfoxides

Hong Liang, Micheline MacKay, T. Bruce Grindley, Katherine N. Robertson, and T. Stanley Cameron

Abstract: X-ray crystallographic studies of two axial glycosyl sulfoxides having R_S configurations (derivatives of phenyl 2-azido-2-deoxy-1-thio-α-D-galactopyranoside *S*-oxide) show that they adopt anti conformations in the solid state, in contrast to previous observations and assumptions. Density functional theory (DFT) calculations at the B3lYP6–311G+(d,p)/6–31G(d) level confirm that anti conformations of both phenyl and methyl R_S glycosyl sulfoxides of 2-azido-2-deoxy-α-D-pyranosides are more stable than exo-anomeric conformations in the gas phase. 1D NOE measurements indicate that the more polar exo-anomeric conformers are only populated to a slight extent in solution. The anti conformations are distorted so that the glycosyl substituents are closer to being eclipsed with H1. This distortion allows S n → σ* overlap if the sulfur lone pair is a p-type lone pair. Evidence for this overlap comes from short C1–S bond distances, as short as the comparable bond distances in the X-ray crystal structure and in the results from DFT calculations for the S_S glycoside, which does adopt the expected exo-anomeric conformation, both in the solid state and in solution, and has normal n → σ* overlap. For 2-deoxy derivatives not bearing a 2-azido group, gas-phase DFT calculations at the same level indicate that the anti- and exo-anomeric conformers have comparable stabilities. Comparison of the results of the two series shows that electronegative substituents in equatorial orientations at C2 destabilize conformations with parallel S–O arrangements, the conformation favored by having an endocyclic C–O dipole antiparallel to the S–O dipole, by about 2.5 kcal mol^{-1} (1 cal = 4.184 J). An equatorial glycosyl sulfoxide, (S_S) phenyl 3,4,6-tri-*O*-acetyl-2-deoxy-2-phthalimido-1-thio-β-D-glucopyranoside *S*-oxide, also adopts an anti conformation in the solid state as shown by X-ray diffraction. It also adopts this conformation in solution, in contrast to studies of other equatorial glycosyl sulfoxides.

Key words: sulfoxide configurations, glycosyl sulfoxides, conformational analysis, density functional theory (DFT) calculations, 1D NOE measurements, X-ray crystallography.

Résumé : Des études de cristallographie par diffraction des rayons-X de deux glycosyles sulfoxydes axiaux de configurations R_S, des dérivés du *S*-oxyde de 2-azido-2-désoxy-1-thio-α-galactopyranoside de phényle, montrent qu'ils adoptent des conformations anti à l'état solide, contrairement aux observations antérieures et aux hypothèses. Des calculs selon la théorie de la fonctionnelle de la densité (TFD) au niveau B31YP6–311G+(d,p)/6–31G(d) confirment que les conformations anti que, en phase gazeuse, chacun des R_S glycosyles sulfoxydes, 2-azido-2-désoxy-1-thio-α-galactopyranoside tant de méthyle que de phényle sont plus stable dans les conformations anomères exo. Des mesures d'effet Overhauser nucléaire (eOn) 1D indiquent que, en solution, les conformères anomères les plus polaires ne forment qu'une faible partie de la population. Les conformations anti sont déformées de façon à ce que les substituants glycolyses soient dans une position pratiquement éclipsée avec le H1. Cette distorsion permet un recouvrement S n → σ* sur la paire libre du soufre est une paire libre de type p. Un support pour ce recouvrement vient des courtes longueurs de liaison C1–S, pratiquement aussi courtes que les longueurs mesurées par diffraction des rayons-X dans la structure cristalline et en accord avec les résultats des calculs TFD pour le S_S glycoside qui adopte la conformation anomère exo attendue, tant à l'état solide qu'en solution, et pour le recouvrement n → σ* normal. Pour les dérivés 2-désoxy ne portant pas de groupe azido, les calculs de TFD en phase gazeuse, au même niveau, indiquent que les conformères anomères anti et exo ont des stabilités comparables. Une comparaison des résultats des deux séries montre que les substituants électronégatifs en orientations équatoriales en C2 déstabilisent les conformations avec des arrangements S–O parallèles, la conformation favorisée par un dipôle C–O endocyclique antiparallèle au dipôle S–O par environ 2,5 kcal mol^{-1} (1 cal = 4.184 J). La diffraction des rayons-X montre aussi que, à l'état solide, un glycosyle sulfoxyde équatorial, le S-oxyde du S_S 3,4,6-tri-*O*-acétyl-2-désoxy-2-phtalimido-1-thio-β-D-glucopyranoside de phényle, adopte aussi une conformation anti. Il adopte aussi cette conformation en solution, en opposition à ce qui a été observé dans les études sur glycosyles sulfoxydes équatoriaux.

Mots-clés : configurations de sulfoxydes, glycosyles sulfoxydes, analyse conformationnelle, calculs selon la théorie de la fonctionnelle de la densité (TFD), mesures d'effet Overhauser nucléaire (eOn) 1D, cristallographie.

Received 3 January 2010. Accepted 11 June 2010. Published on the NRC Research Press Web site at canjchem.nrc.ca on 5 November 2010.

This article is part of a Special Issue dedicated to Professor R. J. Boyd.

H. Liang, M. MacKay, T.B. Grindley,[1] K.N. Robertson, and T.S. Cameron. Department of Chemistry, Dalhousie University, Halifax, NS B3H 4J3, Canada.

[1]Corresponding author (e-mail: Bruce.Grindley@Dal.ca).

Introduction

One of the most important techniques for the formation of glycosides employs glycosyl sulfoxides activated by electrophiles as leaving groups.[1] This method has been used to form glycosides that have widely varying structures for both the glycosyl donors and aglycones.[2–14] The activated sulfoxide is sufficiently reactive that reactions in solution can be conducted at –78 °C and it can also be used in solid-phase reactions.[15] The configuration of the sulfoxide does not influence the stereochemistry of glycosylation reactions but does affect the rate of glycosylation reactions[16] and the rates of competing elimination and hydrolysis reactions.[17,18] The stabilities of the different sulfoxide diastereomers and the physical properties of the diastereomers are inherently linked to the conformations that they adopt. The conformations are termed exo if the aglycone is gauche to both the ring oxygen atom and H1 and anti if the aglycone is anti to the ring oxygen as shown in Figs. 1 and 2. The staggered conformations where the aglycone is gauche to both the ring oxygen and C2 are much less stable and will not be considered here.

It has been assumed that these conformations are influenced primarily by the tendency of the aglycones to adopt exo conformations, the exo-anomeric effect,[19–22] with contributions from repulsion between C–O and S–O dipoles.[23] The exo-anomeric effect is a result of several factors:[24,25] n → σ* donation,[26] dipole dipole repulsion, reduced steric interactions, and electrostatic attraction.[27] Glycosyl sulfoxides provide platforms that allow the examination of the geometrical effects of the contributions of n → σ* donation on conformer stability because the availability of two diastereomers allows the contributions of the two lone pairs to be evaluated individually, albeit with the complication of an additional polar S–O bond. We will show herein that the exo-anomeric effect is much less dominant in controlling the conformations of glycosyl sulfoxides than that of glycosyl sulfides or of normal glycosides and that C–O S–O dipole repulsion is less important than previously thought. We will also show that the conformer stabilities are consistent with the sulfoxide lone pair being a p-type lone pair, rather than an sp^3 lone pair.

Crich et al.[23,28] observed that oxidation of axial thioglycosides on pyranoside rings gave one stereoisomer predominantly, the R_S isomer for α-D-pyranosides. Stereoselectivity is particularly high if the pyranoside rings are made rigid by fusion to 4,6-*O*-benzylidene acetals.[29,30] The stereoselectivity attained is consistent[23] with kinetically controlled oxidation of the accessible face of the sulfur atom in the most stable conformer of the thioglycoside, the conformer favored by the exo-anomeric effect. This group[23] and others[31] observed that oxidation of equatorial sulfoxides was unselective. Khiar et al.[17,26] also found that oxidation of O2-protected equatorial thioglycosides was normally unselective but noted that oxidation of O2-unprotected equatorial thioglycosides is highly diastereoselective. A few O2-substituted equatorial thioglycosides were also found to exhibit highly selective oxidations; peresters of β-thiophenyl or β-ethyl 2-tetrachlorophthalimido-2-deoxy-D-glucopyranosides gave diasteromeric ratios >9:1.[17]

The assignment of configuration of the product sulfoxides has been based on results from X-ray crystallography,[16,17,23,28,32–34] augmented by empirical rules developed from NMR measurements[26] and from the use of chiral shift reagents.[33,35] Khiar[26] proposed two methods for making assignments directly based on NMR results. For ethyl sulfoxides, the methylene protons of the ethyl group are diastereotopic. For equatorial sulfoxides of D-pyranosides, the chemical shift differences between the ^{1}H NMR signals of these diasterotopic protons are considerably larger for the R_S isomer than the S_S isomer.[17,26] This observation has been rationalized in terms of the assumption that the major conformations present for the R_S sulfoxides are those in which the ethyl group adopts the exo orientation,[26] which agreed with results from semiempirical (AM1) calculations.[33] This conformation of the R_S sulfoxides has the sulfoxide sulfur lone pair anti to the C1–O5 bond, aligned so that n → σ* overlap can occur (see Figs. 1 and 2). Crich et al.[23] commented in a footnote that they have observed several exceptions to the tendency for the methylene protons of ethyl sulfoxides to have larger chemical shift differences in particular diastereomers.

The second method proposed for assigning sulfoxide configurations from NMR spectral measurements was based on the ^{13}C NMR chemical shifts of anomeric carbons; those for R_S sulfoxides of equatorial D-pyranosides are more shielded by >2 ppm for both aryl and alkyl sulfoxides.[17,26] For axial sulfoxides of D-pyranosides, the minor S_S isomer exhibits the more shielded anomeric carbon and the larger chemical shift difference between the diastereotopic protons of ethyl sulfoxides.[17] The larger shielding was attributed to the n → σ* overlap mentioned above.[26] If it is assumed that the contribution of conformers with the aglycone gauche to both the ring oxygen and C2 are negligible, this arrangement only occurs in the exo conformation of the equatorial R_S sulfoxide of D-sugars and in the exo conformation of the minor S_S isomer of axial sulfoxides (see Figs. 1 and 2).

Crich et al.[23] have suggested that S–O C1–O5 dipole repulsion is very important in determining the conformations of axial sulfoxides. For α-D-pyranosides, the R_S sulfoxide, which is the major product of oxidation, has the S–O group anti to the ring C1–O5 bond if the conformation adopted is that favored by the exo-anomeric effect. This group has interpreted equilibration results on glycosyl allyl sulfoxides in terms of the importance of dipole–dipole repulsion.[23]

Most of the conclusions about sulfoxide conformation and configuration have been based on X-ray crystallography,[16,17,23,28,32–34] supported by AM1 calculations.[33] With one exception,[23] the ten glycosyl sulfoxides previously studied adopted conformations in the solid state with the sulfoxide alkyl or aryl group in the exo-anomeric conformation. This paper was prompted by our studies of three glycosyl phenyl sulfoxides, all of which adopt conformations in the solid state with the phenyl group anti to the ring C–O bond. We report these crystallographic studies here. In addition, NMR studies have been performed in which NOE buildup rates have been used to determine the preferred conformations of these apparently anomalous sulfoxides in solution. Extensive molecular orbital calculations using density functional theory at the B3LYP6–311+(d,p) level have now provided improved understanding of the factors that determine the relative stabilities of the conformations of the two sulfoxide configurations. These calculations suggest that the

Fig. 1. Exo conformations of the glycosyl sulfoxides of D-sugars in $^4C_1$ chair conformations.

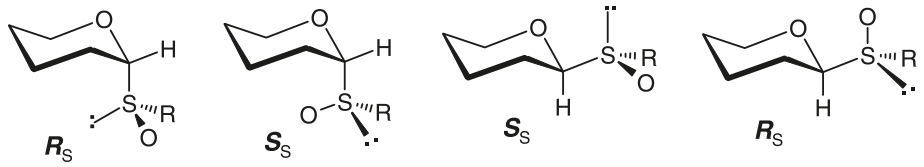

Fig. 2. Anti conformations of the glycosyl sulfoxides of D-sugars in $^4C_1$ chair conformation.

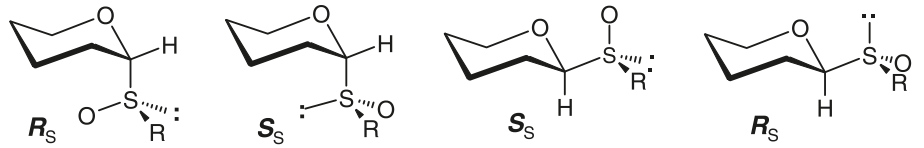

Scheme 1. (a) PhCHO or *p*-MeOPhCHO, *p*-methoxybenzoic acid in DMF–benzene, reflux; (b) Ac_2O/Py; (c) MCPBA, DCM, –78 °C.

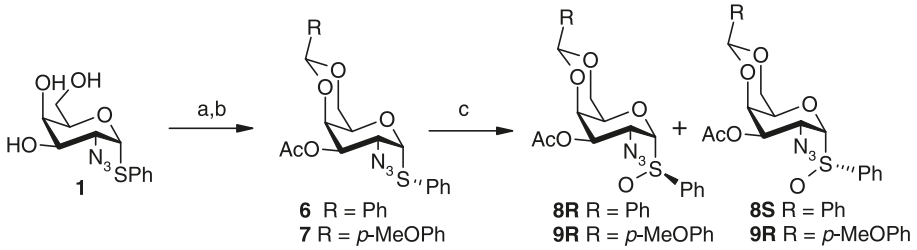

configuration of the glycosyl sulfoxide determines which conformations are populated; a glycosyl sulfoxide, which can adopt a conformation with the aglycone exo and the sulfur lone pair anti, will favor that conformation (the S_S configuration for β-D-pyranosides, the R_S configuration for α-D-pyranosides); for the other diastereomer, the conformer with the aglycone anti is more stable or comparable in stability with the exo conformer.

Results

Axial glycosyl sulfoxides

As previously reported,[36] the treatment of 2-azido-2-deoxy-1,3,4,6-tetra-*O*-acetyl-α-D-galactopyranoside[37] with thiophenol and boron trifluoride etherate in chloroform gave close to a 1:1 mixture of the α- and β-isomers. Deacetylation gave a mixture of compounds **1** and **2** that were separated by column chromatography. As shown in Scheme 1, the α-isomer was converted using standard methods into the 4,6-*O*-benzylidene acetal (**3**) and the 4,6-*O*-*p*-methoxybenzylidene acetal (**5**) that were acetylated to give compounds **6** and **7**, respectively. Compound **3** had been made previously by a different route but was not fully characterized.[38] Oxidation with *m*-chloroperbenzoic acid (MCPBA) in dichloromethane (DCM) at –76 °C yielded two isomeric sulfoxides for the 4,6-benzylidene derivative (**8R** and **8S**) and for the 4,6-*O*-*p*-methoxybenzylidene derivative (**9R** and **9S**). In both cases, the sulfoxide diastereomers were separated by column chromatography. The preferences for the oxidation reactions to yield the R_S isomer were much less than noted for gluco[34,39] and manno[5,29] analogues, being 3/1 for compound **3** and 7/2 for compound **5**.

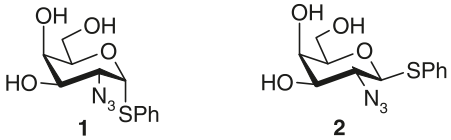

X-ray crystal structure determinations were performed on compounds **6**, **8R**, **8S**, and **9R**. The phenyl thioglycoside, **6**, adopted the exo conformation (Fig. 3). A compilation of all 22 structures previously published that contain axial thioglycosides was assembled from the Cambridge Data File and data from this compilation is listed in the Supplementary data as Table S1. In all previous 22 structures, as well as in the one determined here, the conformation adopted was exo.

The X-ray crystal structure determinations of the kinetically favored sulfoxides **8R** and **9R** show that both adopt anti conformations, different from the exo conformations present in the five previous determinations of axial glycosyl sulfoxides. Two R_S ethyl 1-thio-α-D-mannopyranoside *S*-oxides adopted exo conformations,[28] as did an R_S 2-cyanoethyl 1-thio-α-D-glucopyranoside *S*-oxide,[34] and two 1-thio-β-D-galactofuranoside *S*-oxides with the sulfur atom in pseudo-axial positions also adopt exo-like conformations.[16] ORTEP diagrams for **8R** and **9R** are shown in Figs. 4 and 5. The minor diastereomer, **8S**, adopts an exo conformation in the solid state. Its ORTEP diagram is shown in Fig. 6.

The geometries about the anomeric centre deviate from perfect staggering to different extents in the three axial sulfoxide X-ray crystal structure determinations. The torsional angles are shown in Fig. 7. In the crystal of the parent phenyl thioglycoside, **6**, the quaternary phenyl carbon atom is perfectly staggered between the ring O and H1. In the crys-

Fig. 3. ORTEP diagram of **6**.

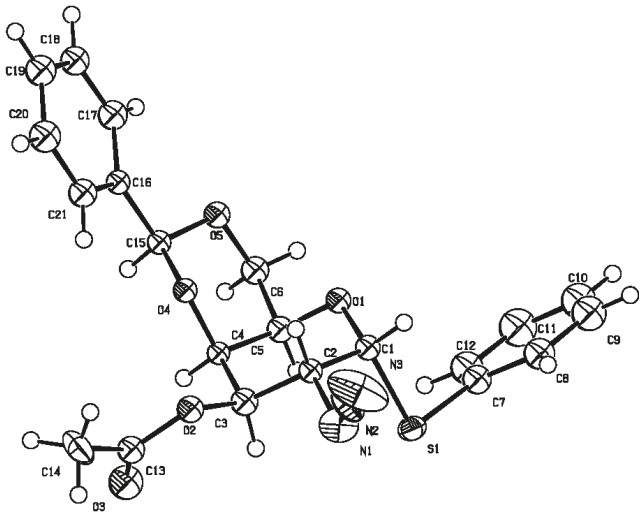

Fig. 4. ORTEP diagram of **8R**.

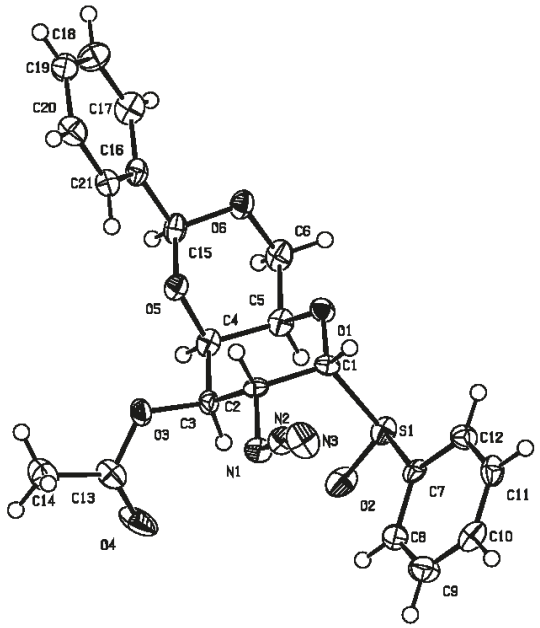

Fig. 5. ORTEP diagram of **9R**.

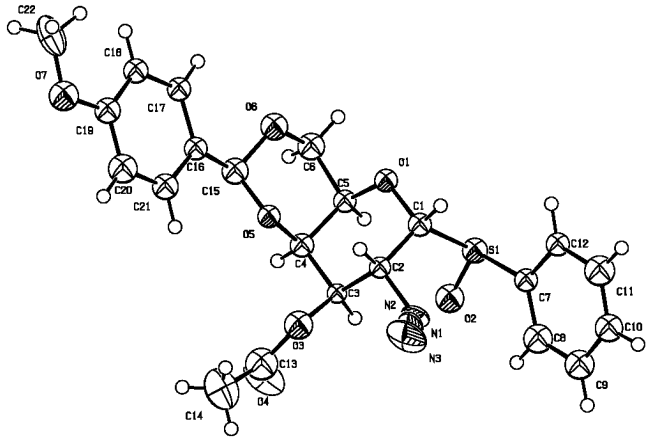

Fig. 6. ORTEP diagram of **8S**.

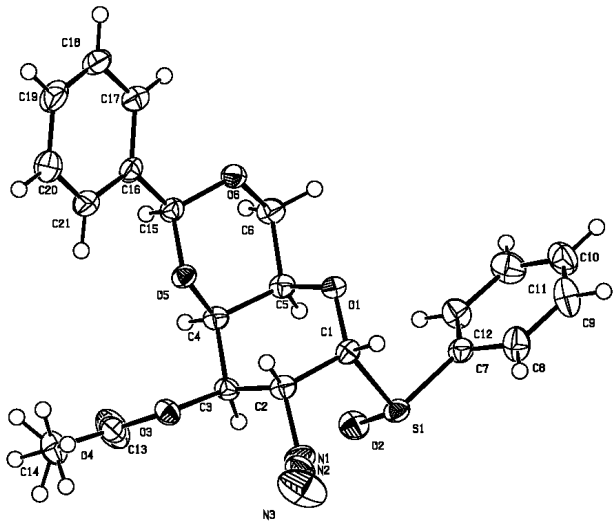

Fig. 7. Newman diagrams from C1 to S indicating torsional angles about the anomeric centres of **6**, **8R**, **8S**, and **9R** calculated for bond angles using the program PLATON.[40] The top two structures have the azide groups in gauche minus conformations, whereas the bottom two are in gauche plus conformations (see the following for further discussion).

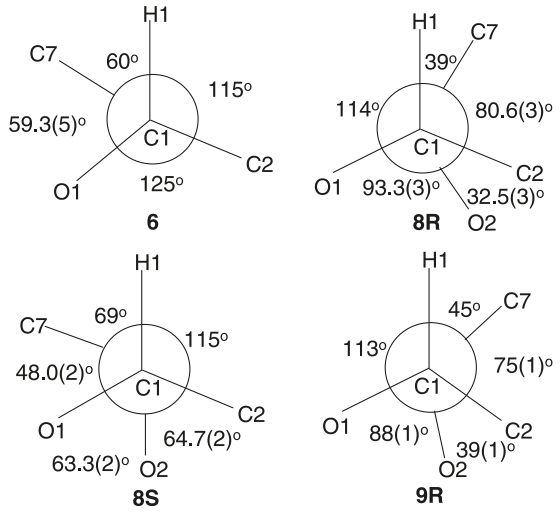

tals of the two sulfoxides that adopt anti conformations, **8R** and **9R**, the quaternary phenyl carbon atom is much further away from C2 than expected for a staggered conformation, having C2–C1–S–C7 torsional angles of 80.6(3)° and 75(1)°, for **8R** and **9R**, respectively. In contrast, in the crystal of the sulfoxide that adopts an exo conformation, **8S**, the quaternary phenyl carbon atom is closer to the ring oxygen (O–C1–S–C7 torsional angle of 48.0(2)°) than expected for a staggered conformation.

Full geometry optimizations were carried out at the B3LYP/6–31G(d) level of theory on the parent phenyl thioglycoside, **6**, its oxides **8R** and **8S**, and their SMe analogs (**10**, **11R**, and **11S**) in the gas phase. Frequency calculations confirmed that all structures identified as conformers were minima on the potential energy surfaces. In these cases, single-point calculations were performed for all conformers

at the B3LYP/6–311G+(d,p) level of theory. The conformational situation is more complicated for these compounds. Rotamer geometries and energies about two torsional angles were evaluated, the glycosidic torsional angle, O5–C1–S–C, and the torsional angle to the azide group, H2–C2–N–N. All other torsional angles were allowed to rotate freely to minimum energy values.

Anti conformations about the C1–S bond of the phenyl thioglycoside, **6**, were not minima on this potential energy surface; initial geometries obtained from a variety of strategies always rotated smoothly back to the exo conformer on minimization. The anti conformer of the methyl analogue **10** was a minimum, 2.30 kcal mol^{-1} (1 cal = 4.184 J) less stable than the exo conformer at the B3LYP/6–31G(d) + ZPVE and 1.70 kcal mol^{-1} less at the B3LYP/6–311G+(d,p) + ZPVE level of theory. Initial geometries for the two additional rotamers about the C2–N bond were obtained by starting from the minimized geometry for each C1–S rotamer and rotating about this bond. Several of these C–N rotamers minimized to previously minimized structures, but two sets of exo and anti minima were obtained for **8R** and **11R**, and one set of two for the exo conformer of **6**. Only one azide rotamer was found for each of the exo and anti conformers of **8S** and **11S**.

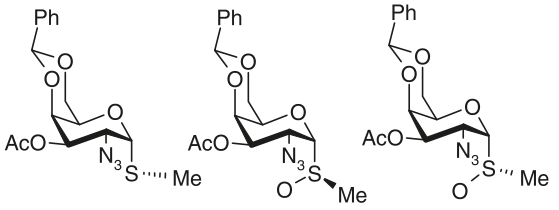

The conformers obtained for **8R** are illustrated in Fig. 8. These are named with the compound number, followed by **e** or **a** to indicate the anomeric conformation (exo or anti, respectively), which is then followed by **a**, **gp**, or **gm**, to indicate whether the azide N–N–C2–H2 torsional angle is anti, gauche plus, or gauche minus, respectively. Conformer stabilities are listed in Table 1.

For the conformers arising because of rotation about the C2–N bond, the gauche plus (**gp**) and gauche minus (**gm**) conformers are calculated to be more stable than the anti (**a**) conformer. The **gp** conformer is always a minimum on the potential energy surface. In the three cases where the **a** conformation is a minimum (**6**, **8R**, **11R**), it is less stable than the **gp** conformer by 1.0 ± 0.2 kcal mol^{-1}. The gauche minus (**gm**) conformer was calculated to be a minimum only for **Re** sulfoxide conformers, **8Re** and **11Re**, but in those two cases, it was calculated to be more stable than the **gp** conformer by 0.7 and 0.9 kcal mol^{-1}, respectively. The azides in the crystal structures of **6** (exo conformer) and **8R** (anti conformer) are present in **gm** conformations, while those in **8S** (exo conformer) and **9R** (anti conformer) are present in **gp** conformations, consistent with the small energy differences between the latter two conformations and probably small barriers between these two minima. The absence of anti conformations for azides in these crystal structures are consistent with the larger energetic destabilizations

Fig. 8. Diagrams indicating the conformations calculated to be adopted by the minima of compound **8R**.

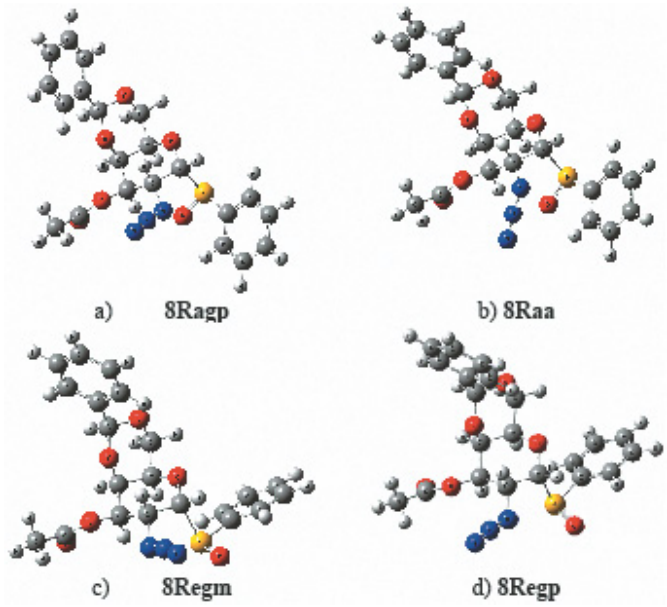

calculated for the **a** conformations with respect to the **gp** conformations. H2–C2–N–N torsional angles were calculated to be small, having absolute values of 38°–46° in all **gp** and **gm** conformers. In the three C–N anti conformers, the H2–C2–N–N torsional angles were between 127° and 147° with the N close to being eclipsed by C3.

The relative energies calculated for the anomeric conformers of these axial glycosyl sulfoxides (Table 1) were unexpected in view of all previous discussion.[17,23,33] The anti conformers of the kinetically favored R_S sulfoxides were calculated to be more stable than the exo conformers by 2.0 and 1.4 kcal mol^{-1} at the B3LYP/6–311G+(d,p) + ZPVE level of theory for the phenyl and methyl sulfoxides, respectively. For the minor sulfoxides, the S_S diastereomers, the exo conformer is calculated to be more stable by 1.1 kcal mol^{-1} for the phenyl glycoside and 2.0 kcal mol^{-1} for the methyl glycoside.

The interesting variations in geometry from perfect staggering around the C1–S bond observed in the X-ray results were evident here for all conformers (see Fig. 9). In particular, the quaternary phenyl carbon atom in the anti conformer of **8R** (**gp**) is calculated to be about as far away from C2 as observed in the crystal, having a C2–C1–S–C7 torsional angle of 81°. In the methyl sulfoxide (**11Ragp**), this angle is calculated to be slightly smaller, 76°. The exo conformers of **8R** are calculated to deviate more from perfect staggering in the unexpected direction than observed in the X-ray structure of **8S**; the O1–C1–S–C7 angle was calculated to be 31° in the most stable **gp** conformer. In the two previously determined X-ray structures of α-D-mannopyranosyl ethyl sulfoxides, the comparable angles observed were larger, 50.7°–56.8°.[28]

In view of the distance determinations obtained from NOE measurements (vide infra) and the difference between calculated and X-ray geometries mentioned earlier, the variations in energy as a function of two different torsional angles were evaluated for compound **8R**. Rotation about the

Table 1. Calculated conformational energies and dipole moments for axial glycosyl sulfoxides.

Conformer	ΔE (6–31G(d)) (kcal mol^{-1})[a]	ΔE (6–31G(d)) (kcal mol^{-1})[b]	ΔE (6–31G(d)) + ZPVE (kcal mol^{-1})[a]	ΔE (6–31G(d)) + ZPVE (kcal mol^{-1})[b]	ΔE (6–311+G(d,p)) + ZPVE (kcal mol^{-1})[a]	ΔE (6–311+G(d,p)) + ZPVE (kcal mol^{-1})[b]	Dipole moment (D)[c]
6egp[d]	0.0	0.0	0.0	0.0	0.0	0.0	1.84
6ea	1.21	1.21	1.28	1.28	1.08	1.08	1.96
10egp	0.0	0.0	0.0	0.0	0.0	0.0	2.24
10agp	2.30	2.30	2.33	2.33	1.70	1.70	0.57
8Ragp	2.03	0.0	2.00	0.0	2.25	0.0	2.54
8Raa	3.04	1.01	3.08	1.07	3.08	0.83	3.31
8Regm	5.36	3.33	5.12	3.12	4.27	2.02	5.55
8Regp	5.97	3.94	5.63	3.62	5.18	2.92	5.73
11Ragp	2.36	0.0	2.42	0.0	2.61	0.0	2.54
11Raa	3.47	1.11	3.58	1.16	3.67	1.05	3.17
11Regm	5.62	3.26	5.29	2.86	4.04	1.42	5.64
11Regp	6.08	3.72	5.62	3.35	5.16	2.54	5.75
8Segp	0.0	0.0	0.0	0.0	0.0	0.0	3.49
8Sagp	1.39	1.39	1.41	1.41	1.08	1.08	2.62
11Segp	0.0	0.0	0.0	0.0	0.0	0.0	3.33
11Sagp	2.45	2.45	2.46	2.46	1.96	1.96	2.99

[a]Relative to the most stable conformer of all diastereomers of this compound.
[b]Relative to the most stable conformer of this diastereomer.
[c]Calculated at the 6–311G+(d,p) level of theory.
[d]No anti conformation of compound **6** was calculated to be a minimum.

Table 2. Comparison of results obtained by different methods.

Compound	Method	Internuclear distance (Å)[a]			Relative energy (kcal mol^{-1})[b]
		$r_{(HSPo,H1)}$	$r_{(HSPo,H3)}$	$r_{(HSPo,H5)}$	
6	NOE	3.0	NO[c]	3.4	NA[d]
	DFT (**egp**)	2.64	5.09	3.40	0.00
	DFT (**ea**)	2.64	5.59	3.46	1.08
	X-ray (**egm**)	2.84	4.78	2.67	NA[d]
8R	NOE	3.0	4.7	3.6	NA[d]
	DFT (**agp**)	2.55	3.84	5.15	0.00
	DFT (**aa**)	2.51	4.17	5.11	0.83
	DFT (**egm**)	2.96	4.12	2.38	2.02
	DFT (**egp**)	2.93	3.96	2.38	2.92
	X-ray (**agm**)	2.68	3.92	5.18	NA[d]
9R	X-ray (**agp**)	2.53	3.86	5.07	NA[d]
8S	NOE	3.4	4.6	3.3	NA[d]
	DFT (**egp**)	2.64	4.66	2.87	0.00
	DFT (**agp**)	3.02	4.76	4.45	1.08
	X-ray (**egp**)	2.95	4.58	2.55	NA[d]

[a]The distance to the closest ortho H (HSPo).
[b]From 6–311G+(d,p) + ZPVE/6-31G(d) calculations.
[c]NO = not observed.
[d]NA = not applicable.

Fig. 9. Newman projections from C1 to S showing torsional angles about the anomeric centre calculated for the various conformers of compounds **6**, **10**, **8R**, **11R**, **8S**, and **11S**.

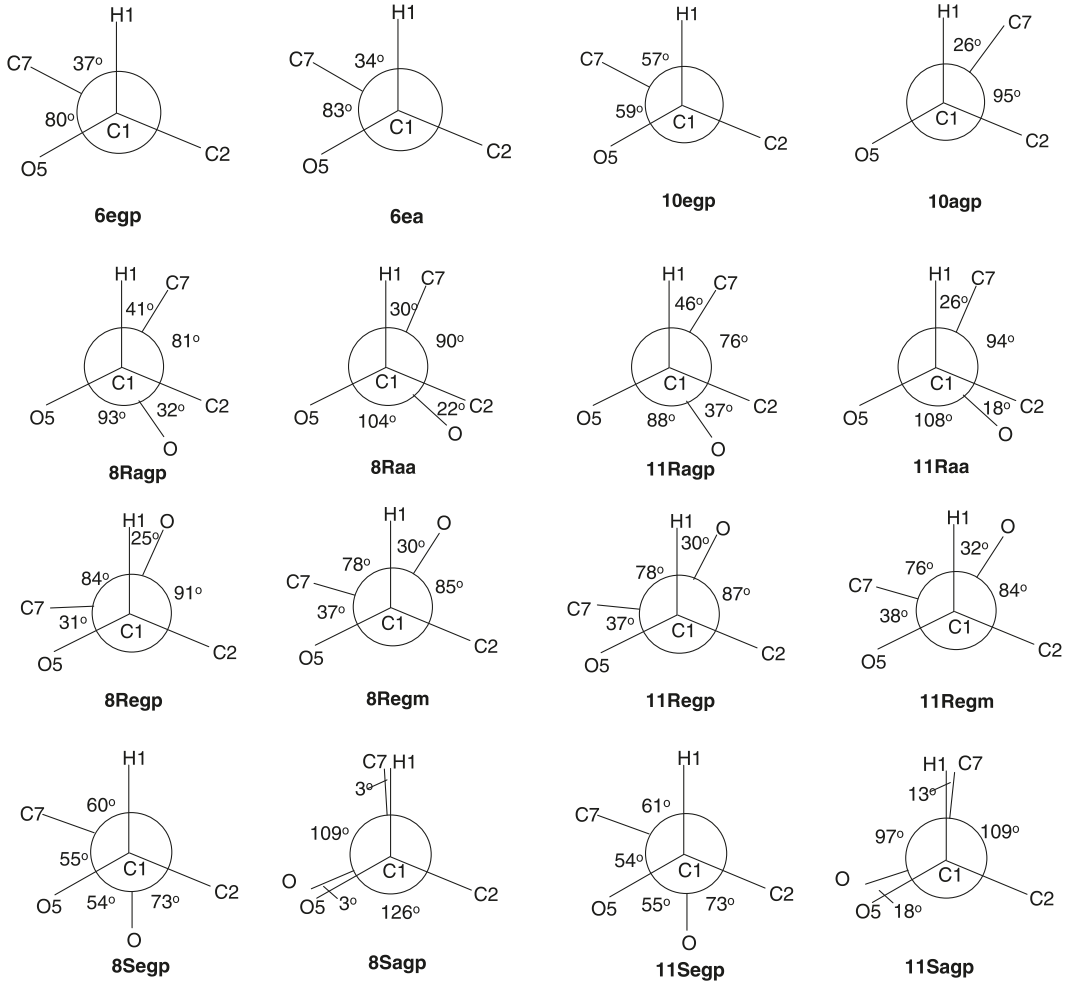

Fig. 10. Variation in energy and internuclear distances calculated using B3LYP6–31G(d) as a function of O5–C1–S–C7 torsional angle for compound **8R**. Right: internuclear distances. Left: energies.

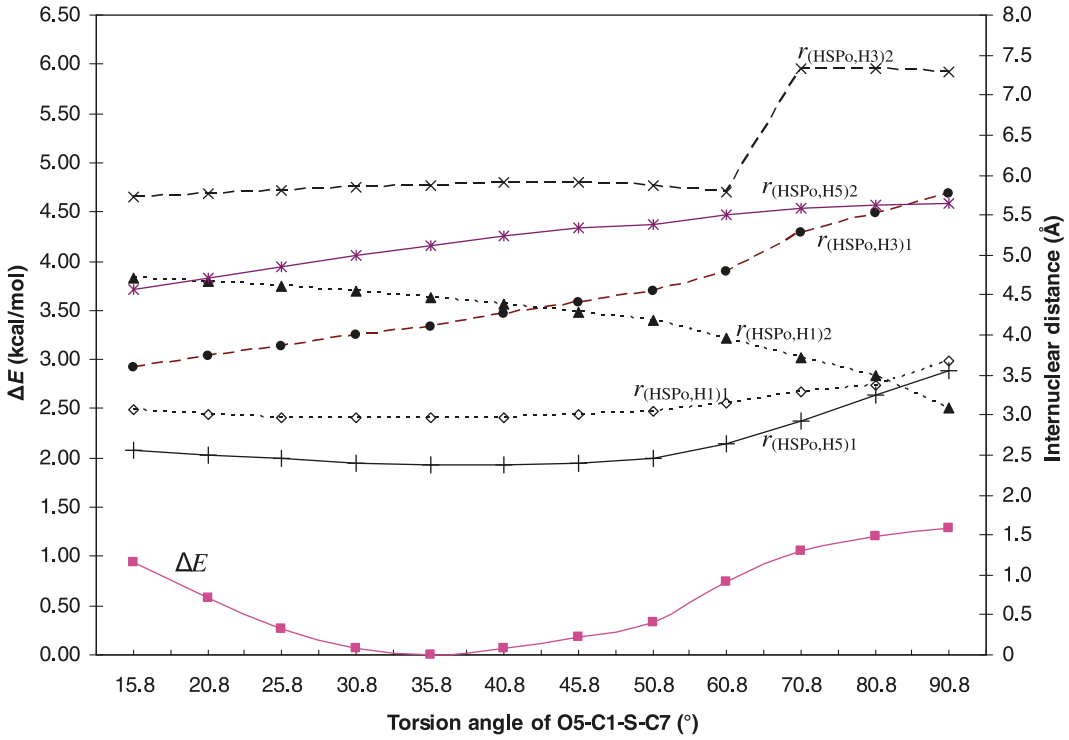

axis of the glycosyl phenyl ring was evaluated first. The torsion angle C1–S–C7–C8 was held constant at fixed values in 10° intervals from the value found at the minimum for the conformer **8Regp**. The energy change as a function of torsional angle is fairly symmetrical about the minima indicating that the measured NOE should represent the minimum well (Fig. S1 in the Supplementary data). Then the torsion angle O1–C1–S–C7 was held constant at values ranging from 5° to 10° increments about the value found at the minimum for the conformer **8Regp**. Figure 10 shows how the energy and the internuclear distances vary as a function of this angle. For torsional angles >90°, the energy decreased in a nonsymmetric way because the azide conformation minimized from the **gm** arrangement was most stable in **8Re** and to the **gp** conformation was most stable for **8Ra**. The variation in energy is not symmetric about this angle, being much flatter towards values of the torsional angle that are larger than that of the minimum. Hence, the time-averaged O1–C1–S–C7 torsional angle will be significantly larger than that present in the geometry of the minimum and the NOEs observed for this conformer and will yield longer H1–HSPo and H5–HSPo distances than calculated for the minimum.

To determine the cause of the method of assignment of sulfoxide configuration based on ^{13}C NMR chemical shifts,[26] the Gauge invariant atomic orbital (GIAO) method[41,42] was used to calculate ^{13}C shieldings for all carbons of the **8R** and **8S** conformers using the 6–311+G(d,p) basis set and 6–31G(d) geometries. TMS was used as the chemical shift reference. The chemical shifts obtained are listed in Table S5 in the Supplementary data and all calculated values were slightly larger than the experimental values. Plots of experimental chemical shifts against the chemical shifts calculated for all nonaromatic carbons gave good straight lines with correlation constants of 0.989–0.996 and slopes ranging from 0.947 to 0.982 (not shown). The anomeric chemical shifts of the carbons consistently deviated from the lines, having calculated values that were larger than the experimental values by greater amounts than those of carbons with similar shifts. According to the method proposed by Khiar,[26] to assign glycosyl sulfoxide stereochemistry from anomeric carbon chemical shifts, C1 of the S_S sulfoxide should be more shielded that that of the R_S sulfoxide. This was observed experimentally: the C1 chemical shifts were 92.5, 96.4, 89.9, and 96.5 ppm for **8S**, **8R**, **9S**, and **9R**, respectively. The values calculated for the four **8R** conformers were 108.9, 112.6, 114.8, and 114.8 ppm for **8Ragp**, **8Raa**, **8Regp**, and **8Regm**, respectively, and those for **8Segp** and **8Sagp** were 106.1 and 105.7 ppm, respectively. Thus, all values for **8S** conformers were less than those for **8R** conformers, which is in agreement with both experiment and prediction. A value for **8R** in between that of **8Ragp** and those of the exo conformers and one for **8S** of the exo conformer would give a difference very similar to those observed in solution for the **8** and **9** diastereomers. Khiar[26] ascribed the shielding of the S_S isomers to n → σ* overlap. The value calculated for C1 of **8Sagp**, which cannot have n → σ* overlap, is the lowest of all, indicating that n → σ* overlap does not cause this shielding effect.

The conformation adopted in solution was investigated by measuring initial NOE buildup rates using both selective 1D NOE measurements with the double pulsed field gradient spin echo (DPFGSE) sequence[43] and 2D NOESY experiments using a variety of mixing times. The initial rates are directly proportional to the internuclear distances (r_{IS}) and were calibrated using a known internuclear distance (r_{ref}) as follows:

$$r_{IS} = r_{ref}\left(\frac{NOE_{ref}}{NOE_{IS}}\right)^{1/6}$$

The distance between ortho phenyl protons (HSPo; 2.8 Å) was used as the reference distance (r_{ref}).[44] The results are given in Table 2 along with the results obtained by the previous methods.

For the parent compound **6**, the NOE results fit the geometry calculated for the exo conformer well. The distances from HSPo obtained to H1 and to H5 are within 0.4 Å of those calculated and no NOE was observed for the interaction with H3, as expected. However, the H5–HSPo distance obtained from the NOE measurement was much longer than that measured from the X-ray results. As discussed previously, the potential surface is fairly flat with respect to changes in the O1–C1–S–C7 torsional angle from the 80° value calculated for the gas phase. Crystal packing presumably causes this value to be altered from that calculated for the minimum to the 59.4(5)° value observed in the solid state. The average of all 23 O1–C1–S–C7 torsional angles from the crystal structures in the Cambridge data file (Table S1 in the Supplementary data) was 61.5°.

For the R_S sulfoxide, the distances obtained from the NOE measurements do not match the pattern obtained from the X-ray results or from the geometries calculated for the two lowest energy minima, the global minimum, the **8Ragp** conformer, and the other anti conformer (see Table 2). In both anti conformers, the H5–HSPo distance is calculated by DFT to be >5 Å, too large to give an NOE. However, an H5–HSPo NOE was observed and the distance calculated from it was 3.62 Å. For both exo conformers, the H5–HSPo distances are calculated by DFT to be 2.38 Å, much shorter than the distance obtained from the NOE. The H1–HSPo distance, obtained from the NOE, was 3.05 Å. The average of DFT calculated values in the two exo conformers is 2.95 Å and is 2.53 Å in the two anti conformers. These results indicate that a mixture of the exo and anti conformers is present in solution.

A very approximate estimate of the amount of the exo conformer present can be obtained from the H5–HSPo distances calculated for exo and anti conformers and the value obtained from the NOE measurement using r^6 averaging. The use of 3.6 Å for the average, 5.15 Å for the anti conformer, and 2.38 Å for the exo conformer yields 7% of the exo conformer. This amount corresponds to a ΔG° value of 1.5 kcal mol^{-1} for the equilibrium between conformers, which is on the same order as that calculated.

Evaluation of the effect of the 2-azido group

To examine whether the above results were influenced by the 2-azido group, calculations were performed on the 2-deoxy analogs shown below at the same level of theory, except that conformations were also minimized at the B3LYP/6–311+G(d,p) level. As previously, calculations were performed on two conformations of each of these, the anti (**a**) and exo (**e**) conformers. In addition, calculations were performed on the endo conformers of the methyl glycosyl sulfoxides, **15Sen** and **15Ren**, to check whether the earlier assumption that this class of conformer was too energetic to contribute to the mixture present was valid. The anti conformers of both S_S diastereomers, that is, **13Sa** and **15Sa**, were not minima on their potential energy surfaces and neither was one of the endo conformers, **15Ren**. The results are given in Table 3 and Newman projections showing the relationships among groups at the anomeric centres are shown in Fig. 11.

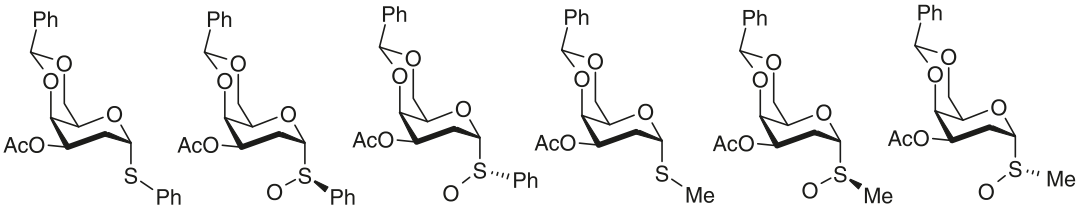

The exo conformer of the methyl 2-deoxythioglycoside (**14**) was calculated to be somewhat more stable with respect to the anti conformer than its 2-azido-2-deoxy analogue (**10**) (3.2 vs 2.3 kcal mol^{-1}). For this series, the anti conformer of the phenyl thioglycoside was also a minimum, 2.3 kcal mol^{-1} less stable than the exo conformer. For the R_S sulfoxide of the 2-deoxy analogue, **15**, the exo conformer (**15e**) was more stable than the anti conformer (**15a**) by 1.5 kcal mol^{-1}. The two conformers of the R_S phenyl 2-deoxy sulfoxides (**13**) were calculated to be almost equally stable at the B3LYP 6–311+G(d,p) level of theory, the exo conformer being 0.1 kcal mol^{-1} more stable. Neither of the anti conformers of the S_S sulfoxides of the 2-deoxy derivatives (**13Sa** and **15Sa**) were minima at this level of theory.

As shown in Fig. 11, the C2–C1–S–C7 torsional angles in the anti conformers of the R_S sulfoxides are similar to those of their 2-azido analogues; the values are greater than those expected for perfect staggering, being 70° for **R13a** and 78° for **R15a**. In contrast, the exo conformers of **R13** and **R15** deviate from perfect staggering in the opposite direction from their 2-azido analogues. In the latter derivatives (see Fig. 9), the O5–C1–S–C7 torsional angle had values in the 31°–38° range, whereas the O–S–C1–C2 angle was in the 84°–91° range. For **13Re** and **15Re**, the values of the O5–C1–S–C7 torsional angles are 82° and 71°, respectively, whereas those of the O–S–C1–C2 angles are 41° and 52°, respectively. These changes are consistent with relief of dipole–dipole repulsion between the potentially parallel C–N and S–O dipoles of the 2-azido derivatives. When the 2-azido group was removed, the conformational minima have O–S–C1–C2 angles <60° and the O5–C1–S–C7 values are >60°, relieving steric strain from the interaction of the aglycone with the pyranose ring.

Table 3. Calculated conformational energies and dipole moments for axial 2-deoxyglycosyl sulfoxides.

Conformer	ΔE (6–31G(d)) + ZPVE (kcal mol^{-1})[a]	ΔE (6–311+G(d,p)) + ZPVE (kcal mol^{-1})[a]	Dipole moment (D)[b]
12e	0.0	0.0	0.98
12a	2.45	2.26	2.55
13Re	0.29	0.0	2.96
13Ra	0.0	0.08	3.76
13Se	0.84	0.45	3.29
14e	0.0	0.0	0.78
14a	3.22	3.16	2.24
15Re	0.37	0.0	3.18
15Ra	1.34	1.54	3.33
15Se	0.0	0.14	3.32
15Sen	5.82	5.25	3.75

[a]Relative to the most stable conformer of all diastereomers of this compound.
[b]Calculated at the 6–311G+(d,p) level of theory.

Fig. 11. Newman projections from C1 to S showing torsional angles about the anomeric centre calculated for the conformers of compounds **12R**, **12S**, **13R**, **13S**, **14R**, **14S**, **15R**, and **15S**.

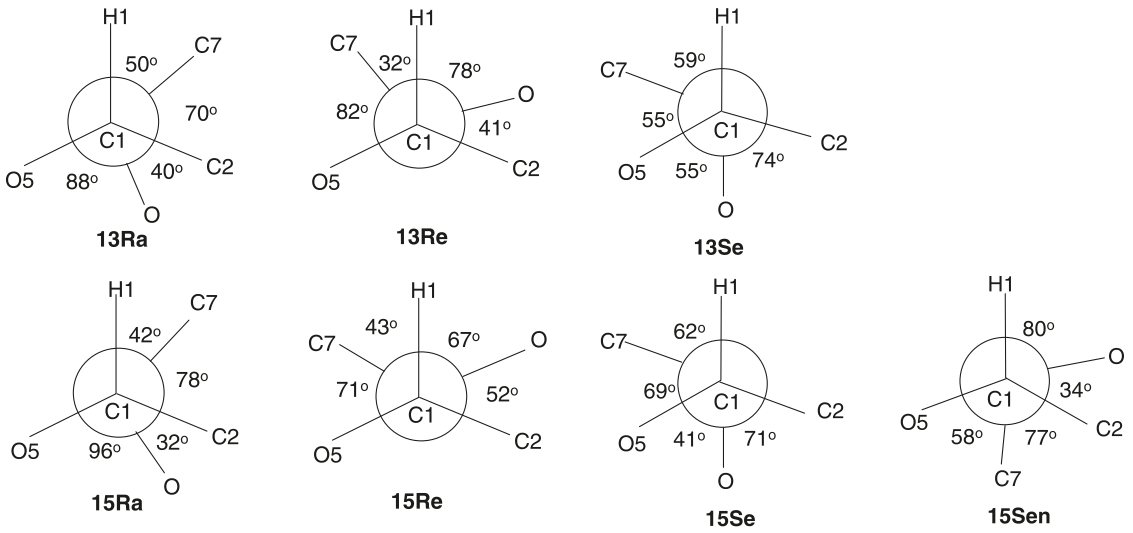

An equatorial glycosyl sulfoxide

Treatment of 1,3,4,6-tetra-*O*-acetyl-2-deoxy-2-phthalimido-β-D-glucopyranoside[45–47] (**16**) with thiophenol and boron trifluoride etherate gave phenyl 3,4,6-tri-*O*-acetyl-2-deoxy-2-phthalimido-1-thio-β-D-glucopyranoside (**17**), previously prepared by another method,[48] in an 81% yield. Oxidation with 1 equiv of *m*-chloroperbenzoic acid in dichloromethane at –78 °C yielded 92% of a 2.1:1 mixture (**18**) of the S_S (**18S**) and R_S (**18R**) isomers. It had previously been reported that oxidation under similar conditions gave a 3:1 ratio of the same isomers.[17] The isomers were separated using flash chromatography on silica gel with 5% acetone in dichloromethane as eluent.

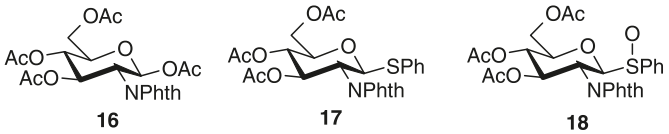

The major isomer (**18S**), the S_S isomer, was recrystallized from a solution of 1% ethanol in hexanes. Its crystal structure (Fig. 12) establishes the S_S configuration. Interestingly, the compound adopts the conformation with the phenyl group anti to the C1–O5 bond, in contrast to the results from all previous X-ray determinations of equatorial glycosyl sulfoxides except one[23] (see Table S1 in the Supplementary data for data on previous X-ray determinations of glycosyl sulfoxides). In this conformation, the phenyl and phthalimido groups lie roughly parallel to each other and perpendicular to the plane of the tetrahydropyran ring, in an arrangement typical of π stacking.

This conformation of **18S** persists in solution in chloroform-*d*. The nearly parallel alignment of the aryl groups is evident in both the chemical shifts of the phenyl protons and of the phthalamido protons, which are affected by the anisotropic chemical shift effects of these aryl groups (for recent summaries of these effects, see papers by Lazzeretti and coworkers[49,50]). In the ^{1}H NMR spectrum of the starting material (**17**), the phenyl ortho Hs appear at 7.45 ppm, whereas the meta and para Hs appear as a complex multiplet from 7.2 to 7.3 ppm. Similar shifts have been reported for cyclo-

Fig. 12. ORTEP diagram of **18S**.

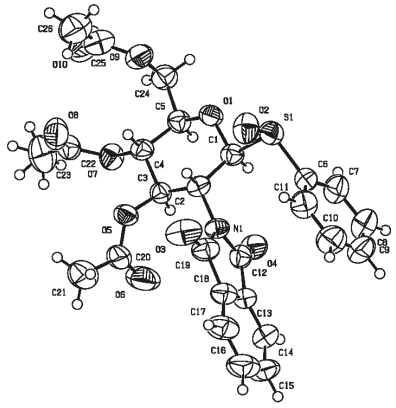

hexyl phenyl sulfide, 7.38 (ortho), 7.25 (meta), and 7.17 (para) ppm.[51] Conversion to the sulfoxide results in deshielding, e.g., in the spectrum of cyclohexyl phenyl sulfoxide, 7.54 (ortho), 7.45 (meta), and 7.45 (para) ppm,[51] and also in that of compound **18R**, 7.90 (ortho), 7.58 (meta), and 7.70 (para) ppm (see Fig. 13). In contrast, in the ^{1}H NMR spectrum of **18S**, these signals appear at 7.49 (ortho), 7.21 (meta), and 7.13 (para) ppm (Fig. 14). All signals are shielded in comparison with those of the R_S isomer, $\Delta\delta$ 0.41 (ortho), 0.37 (meta), and 0.57 (para) ppm, which are consistent with the effects of a nearly parallel phthalimido group.

The effects on the phthalimido protons are more dramatic. AA′BB′ patterns typical of disubstituted benzenes with identical ortho substituents are observed for the parent compound with chemical shifts of 7.76 and 7.87 ppm and for **18R** with chemical shifts of 7.77 and 7.90 ppm (Fig. 13). In contrast, the phthalimido proton signals in the spectrum of **18S** are exchange broadened (Fig. 14). A broad singlet at 7.67 ppm is superimposed on a much broader smooth low band centered at about 7.73 ppm. Rotation of the phthalimido group is hindered by the favorable interactions associated with the near parallel arrangement of the phenyl and phthalimido groups. If there was a rapid equilibrium between anti and exo conformations, the phthalimido group would be able to rotate freely when the phenyl group was exo. Thus, the observation of a single pattern exhibiting hindered rotation indicates that the anti conformation is essentially the only conformation populated in solution and that rotation about the C1–S bond to the exo conformation is slow, as are rotation about both the phenyl C–S bond and the C2–N bond.

Quantum mechanical calculations were performed with density functional theory as implemented in Gaussian 03[52] with Becke's three parameter exchange functional and Lee–Yang–Parr correlational functionals.[53,54] The X-ray structure of compound **18S** provided the initial geometry of the glycosyl sulfoxide. The initial geometries for the second staggered rotamer were generated by rotating about the C1–S bond and those for the other sulfoxide diastereomer were generated by inverting at sulfur. The third staggered rotamer, with the aglycone gauche to both C2 and the ring oxygen, was not used as a starting point for geometry minimization. Initial geometries for the SMe analog and its sulfoxides were obtained from the minimized thiophenyl conformers. Initial geometries for **17** and its methyl ana-

Fig. 13. Part of the 400 MHz ^{1}H NMR spectrum of compound **18R**.

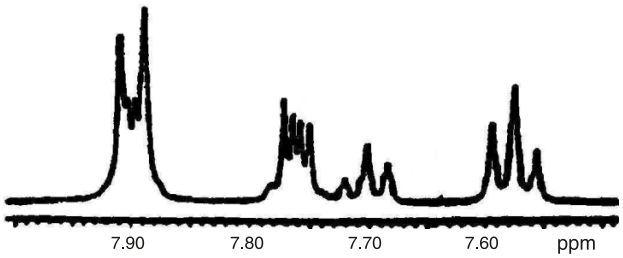

Fig. 14. Part of the 400 MHz ^{1}H NMR spectrum of compound **18S**.

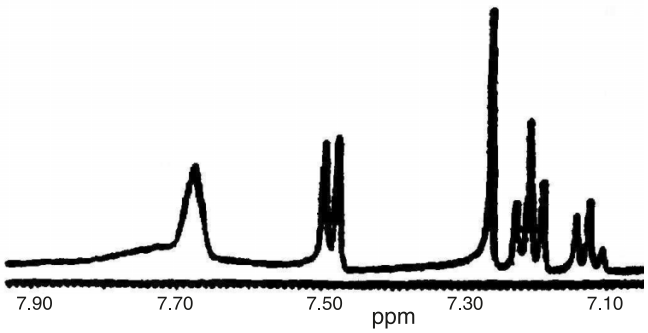

logue, **17Me**, were obtained by removing an oxygen atom from the minimized sulfoxide conformers. Full geometry optimizations were carried out at the B3LYP/6–31G(d) level of theory on **17**, **18S**, and **18R**, and their SMe analogs (**17Me**, **18SMe**, and **18RMe**). However, neither Hartree–Fock molecular orbital theory nor current implementations of density functional theory, which use local approximations of the density, are capable of accurately describing the dispersion forces, which are the major interaction causing π stacking.[55] Theoretical methods that could provide accurate measures of the dispersion forces are too time-consuming for molecules of the size of compound **18S**. Thus, the stabilities of conformers with geometries in which two arene rings are close to parallel will be underestimated.

All starting conformations, that is, both anti and exo conformations, of the parent thioglycosides, **17** and **17Me**, smoothly changed geometry on optimization to that of the exo conformers. On this potential energy surface, the anti conformations are not minima. The results for the glycosyl sulfoxides are shown in Table 4. The most stable conformer of the S_S diastereomer is calculated to be more stable than that of the R_S diastereomer by 1.85 and 1.36 kcal mol^{-1} for the phenyl and methyl glycosyl sulfoxides, respectively. For all compounds, the exo conformers are calculated to be more stable than the anti conformers. For **18S**, which was observed to adopt the anti conformer both in the solid state and in solution, the exo conformer was calculated to be the more stable conformer by 1.57 kcal mol^{-1}, although the anti conformer is calculated to have the larger dipole moment, 5.63 vs 1.40 D. For **18R**, which is present as the exo conformer in solution, the calculated difference is 3.03 kcal mol^{-1}.

Table 4. Calculated conformational energies and dipole moments for the equatorial glycosyl sulfoxides.

Conformer	ΔE (6–31G(d)) (kcal mol^{-1})[a]	ΔE (6–31G(d)) (kcal mol^{-1})[b]	Torsional angle O5–C1–S–C (°)	Torsional angle O5–C1–S–O (°)	Dipole moment (D)[c]
18Santi	1.57	1.57	–157.7	91.4	5.63
18Sexo	0.0	0.0	–67.6	–177.1	1.41
18Ranti	3.03	4.88	–176.1	–66.5	6.60
18Rexo	0.0	1.85	–54.2	56.7	4.00
18SMeanti	2.31	2.31	–145.1	103.7	4.61
18SMeexo	0.0	0.0	–65.5	–175.3	0.86
18RMeanti	3.48	4.83	–168.4	–59.4	6.46
18RMeexo	0.0	1.36	–44.9	66.4	3.85

[a]Relative to the most stable conformer of all diastereomers of this compound.
[b]Relative to the most stable conformer of this diastereomer.
[c]Calculated at the 6–31G(d) level of theory.

Discussion

Axial glycosyl sulfoxides

The gas phase DFT calculations indicate that axial glycosyl sulfides favor the exo-anomeric conformers over anti conformers by substantial amounts, 1.7 kcal mol^{-1} for the methyl 2-azido-2-deoxythioglycoside (**10**) and 3.2 kcal mol^{-1} for the methyl 2-deoxythioglycoside (**14**). For the phenyl 2-azido-2-deoxythioglycosides, the anti conformations were not minima on the potential energy surfaces. The fact that in all 23 X-ray structure determinations of axial glycosyl sulfides, the conformation observed was the exo conformation (Table S3 in the Supplementary data) confirms these calculated results.

Of the two diastereomers of the glycosyl sulfoxides, **8** and **11**, the most stable conformer of the minor diastereomers, **8S** and **11S**, are calculated to be more stable than that of the major diastereomers by 2.3 and 2.6 kcal mol^{-1}, respectively. Because the diastereomers obtained to a greater extent from the oxidation are calculated to be less stable than the diastereomers obtained in lesser amounts, this result strongly supports the conclusion that the stereoselectivity of oxidation is kinetically controlled and results from the preferred exo conformation of the sulfide.[23,28]

The 2-azido-2-deoxy S_S sulfoxides (**8S** and **11S**), which retain the sulfur lone pair anti to the C1–O5 bond in the exo conformers, were calculated to have about the same conformational preferences for these exo conformers as the parent sulfides. One factor favoring this conformer must be n $\rightarrow$ σ^* donation from the sulfur lone pair into the C1–O5 antibonding orbital. This conformer is calculated to have the shortest C1–S bonds of all conformers of **8** and **13** (see Fig. 15), which is consistent with this overlap. Thus, the exo arrangement of the aglycone plus the n $\rightarrow$ σ^* overlap helps explain the greater stability of this conformer of the kinetically disfavored diastereomer.

However, for the R_S sulfoxide (**11Ragp**), which does not have an anti lone pair in the exo conformation, the conformational preference is calculated to shift from being in favor of the exo conformer for the parent methyl sulfide (**10egp**) by 1.7 kcal mol^{-1} to being in favor of the anti conformer by 1.4 kcal mol^{-1}, a change of 3.1 kcal mol^{-1} (3.7 kcal mol^{-1} for the phenyl glycoside, if it is assumed that the sulfide preference is the same as for the methyl glycoside). For the R_S sulfoxide of the 2-deoxy analogue, **15**, the exo conformer (**15e**) was more stable than the anti conformer (**15a**) by 1.5 kcal mol^{-1}. Therefore, the extent to which the anti conformer of the methyl thioglycoside was stabilized on oxidation to the R_S diastereomer was smaller for the 2-deoxy derivative, 1.5 kcal mol^{-1}, but was still substantial. For the phenyl thioglycoside (**12**), the corresponding stabilization of the anti conformer of the R_S sulfoxide was calculated to be 2.2 kcal mol^{-1}, again at the B3LYP 6–311+G(d,p) level of theory.

Comparison of the geometries of the R_S exo conformers of the 2-deoxy derivatives with the 2-azido-2-deoxy derivatives shows that the 2-azido substituent has a significant effect. The O5–C1–S–O torsional angles calculated for **8Regp**, **8Regm**, **11Regp**, **11Regm**, **13Re**, and **15Re** are 139.3°, 144.4°, 145.0°, 146.2°, 168.5°, and 179.5°, respectively. The latter two values are consistent with minimization of steric interactions for the R group and dipole–dipole repulsion due to interaction of the endocyclic C–O bond and the sulfoxide S–O bond. When the 2-azido group is present, dipole–dipole repulsion between the parallel C2–N bond and the S–O bond causes rotation about the C1–S bond resulting in much smaller O5–C1–S–O torsional angles. This is a significant effect because it is at the expense of increased R pyranose ring steric interactions and increased dipole–dipole repulsion due to interaction of the endocyclic C–O bond and the sulfoxide S–O bond. The small effect of the latter type of dipole–dipole repulsion suggests that it is not as important as other factors in determining conformational preferences for glycosyl sulfoxides.

In terms of energies, the most stable azide conformers of the anti R_S 2-azido-2-deoxy derivatives are calculated to be more stable than the most stable azide conformers of the exo R_S 2-azido-2-deoxy derivatives by 2.0 and 1.4 kcal mol^{-1} for the phenyl and methyl sulfoxides, respectively, at the B3LYP6–311+G(d,p) level of theory. For the 2-deoxy derivatives, without the parallel C–N dipole, the exo conformers are now more stable by 0.1 and 1.5 kcal mol^{-1} for the phenyl and methyl sulfoxides, respectively. This represents changes of 2.1 and 2.9 kcal mol^{-1} for the phenyl and methyl sulfoxides, respectively, and represents the costs of having these dipoles parallel.

Fig. 15. Calculated structural features for axial phenyl sulfide and phenyl sulfoxide conformers.

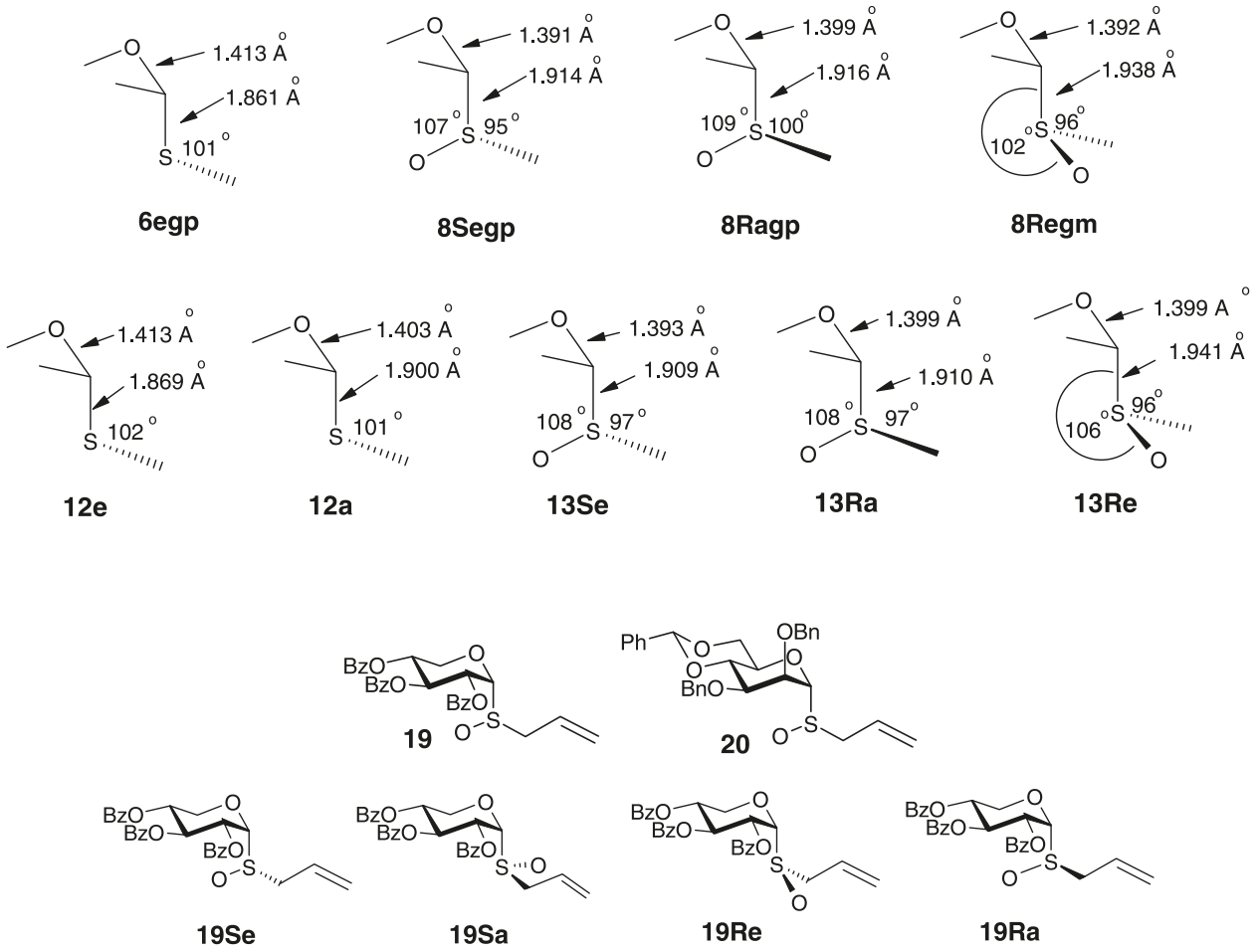

Crich et al.[23] equilibrated the two sulfoxide diastereomers of allyl 2,3,4-tri-*O*-benzoyl-1-thio-α-D-xylopyranoside oxide (**19**) and allyl 2,3-di-*O*-benzyl-4,6-*O*-benzylidene-1-thio-α-D-mannopyranoside oxide (**20**) in both benzene-d_6 and methanol-d_4 at 60 °C. The former compound is most analogous to those studied here because in its $^4C_1$ conformation it bears an equatorial substituent at C2. For **19**, the S_S diastereomer was favored by 2 to 1 in benzene but the other diastereomer was favored by 2.5 to 1 in methanol. The results here indicate that **19S** will prefer the exo conformation, **19Se**, rather than the anti conformation, **19Sa**, because this allows the allyl group to assume the sterically preferred exo orientation and because the sulur lone pair is correctly oriented for n → σ* overlap. Crich et al.'s[23] results do not provide a direct estimate of the preference for the S_S diastereomer because the R_S diastereomer ring inverts completely (as determined from $^3J_{H,H}$ values) to the $^1C_4$ chair. To compare relative stabilities of particular conformers of the S_S and R_S diastereomers, the same ring conformations must be employed. If the conformational preference for $^1C_4$ over $^4C_1$ is estimated at >9/1, the equilibration results for **19** correspond to ΔG° values of >1.9 and >0.8 kcal mol^{-1} at 60 °C in benzene and methanol, respectively, in favor of the S_S diastereomer in the $^4C_1$ conformation. The value in benzene is in the same range as that calculated by DFT methods here (**11Segp** is calculated to be 2.4 kcal mol^{-1} more stable than **11Ragp**), even though the C2 substituent is very different. Since the S_S diastereomers are calculated to have somewhat larger dipole moments (3.3 vs 2.5 D for **18**, 3.5 vs 2.5 D for **11**), the decreased preference for this diastereomer in methanol is unexpected and may be due to specific solvation of the R_S diastereomer as suggested by Crich et al.[23]

For compound **20**, the preferences for the R_S diastereomer are 0.7 and 0.6 mol^{-1} at 60 °C in benzene and methanol, respectively. Using the value estimated previously, this result indicates that the R_S diastereomer is stabilized by >2.6 kcal mol^{-1} when the equatorial 2-*O*-benzoyl group is converted to axial. Comparison of the calculated relative stabilities of the analogous 2-azido-2-deoxy diastereomers (**11**) with their 2-deoxy analogs (**15**) shows a similar 2.5 kcal mol^{-1} relative stabilization of the R_S diastereomer on removal of the equatorial 2-azido group. From these results, it is clear that the C2 configuration has a large effect on diastereomer stability.

It remains to be considered why the anti conformers of the R_S sulfoxides are more stable relative to the exo conformers than expected based on normal[23] conformational arguments. It is very well established that glycosides and thioglycosides prefer exo-anomeric conformations. Several factors influence this preference: n → σ* overlap, dipole–

dipole repulsion, and reduced steric interactions and electrostatic attraction. Changing from a sulfide in the exo-anomeric conformation to the R_S sulfoxide results in the loss of the n → σ* overlap but adds a dipole in its most favorable arrangement with respect to the endocyclic C1–O5 dipole, namely, antiparallel. However, in **8Re** and **11Re**, it also adds a parallel dipole–dipole repulsive interaction between the S–O dipole and the C2–N dipole. As noted previously, the anti conformers have C2–C1–S–C7 torsional angles that are considerably greater than staggered, both in the presence and absence of electronegative substituents on C2. This deviation from perfect staggering has the effect of minimizing steric interactions at the expense of increasing dipole–dipole repulsion between the S–O bond and the endocyclic C–O bond. Clearly, the latter factor is less important than the former and any other interactions. It is interesting that the C7–S–O units in the anti conformers are close to being eclipsed by the H1–C1–C2 unit (see Fig. 13, **8Ra** and **11Ra**, and Fig. 12, **13Ra** and **15Ra**). If they were eclipsed, the sulfur lone pair would be syn to the C1–O5 bond. The C1–S bonds in the most stable **Ra** conformers, **8Ragp** and **13a**, are calculated to be almost as short as they are in the conformers having n → σ* overlap, **8Sepg** and **13Se**, which is consistent with an extra stabilizing interaction. This interaction is between orbitals of correct symmetry if the S lone pair that overlaps with the C1–O5 σ* orbital is a p-type lone pair. All of the other conformers are calculated to have C1–S bond lengths that are 0.02–0.05 Å longer (see Fig. 15). Based on a perturbation molecular orbial (MO) approach for dimethoxymethane,[56] Tvaroška and Bleha[21] have concluded that both the σ and π lone pairs on oxygen can overlap with the C–O σ* orbital and both overlaps provide similar stabilization. The overlap advocated here is similar to the oxygen atom π → σ* overlap of that view.[21]

Comparison of the **Re** and **Se** conformers of the 2-deoxy derivatives allows an evaluation of the relative strengths of n → σ* overlap and adoption of antiparallel endocyclic C–O and S–O dipoles (see Fig. 12 for Newman projections of the relevant relationships). The **Re** conformers have antiparallel endocyclic C–O and S–O dipoles. The **Se** conformers adopt shapes with ideal geometries for n → σ* overlap but are presumably destabilized by gauche interactions between endocyclic C–O and S–O dipoles. For both the phenyl and methyl sulfoxides, the **Re** conformers are calculated to be slightly more stable, by 0.45 and 0.14 kcal mol^{-1}, respectively, suggesting that the two interactions are comparable in magnitude.

Equatorial glycosyl sulfoxides

Equatorial alkyl and aryl thioglycosides overwhelmingly adopt exo-anomeric conformations in the solid state (22 out of 25, see Table S1 in the Supplementary data), indicating that there is a strong thermodynamic preference for this conformation. The results of DFT (6–31G(d) B3LYP) calculations support this conclusion, since the anti conformations of both the thiophenyl and thiomethyl glycosides smoothly change geometry on minimization to the exo conformer, although this level of theory underestimates[55] the stabilizing effect of π stacking.

In contrast, (S_S) phenyl 3,4,6-tri-*O*-acetyl-2-deoxy-2-phthalimido-1-thio-β-D-glucopyranoside *S*-oxide (**18S**) adopts the anti conformation about the glycosidic linkage in the solid state and the NMR evidence described in the Results section demonstrated conclusively that this conformation is the predominant one in solution. The near parallel alignment of the SPh and phthalimido groups suggests that π stacking contributes to the stabilization of this conformation. π Stacking was recently shown to influence the conformation about the glycosidic bond in a disaccharide.[57] Such interactions provide stabilizations on the order of 2.8 kcal mol^{-1} for the most favorable displaced parallel geometries.[55,58–61] This factor is presumably very important in causing compound **18S** to adopt the anti conformation. It is notable that compound **18R**, which could also adopt a π-stacked conformation, clearly adopts the conformation favored by the exo-anomeric effect (as shown by its NMR spectra data) with the phenyl group exo and the lone pair on sulfur correctly aligned for n → σ* overlap with the C1–O5 antibonding orbital.

The DFT calculations for the glycosyl sulfoxides indicate that the exo conformers of both diastereomers are more stable in the gas phase. For the phenyl glycosyl sulfoxides, the differences are calculated to be 1.57 and 3.03 kcal mol^{-1} for **18S** and **18R**, respectively. The **18R** exo conformer is stabilized by having the S lone pair anti to the ring C–O bond, which is geometry suitable for n → σ* overlap. This conformer is calculated to have the shortest C1–S bond length, 1.878 vs 1.885 Å for the **18S** exo conformer and >1.89 Å for the anti confomers, which is in agreement that this overlap is significant.

Even though the conformation adopted by the S_S diastereomer is not that predicted on the basis of the exo-anomeric effect, the ^{13}C NMR chemical shift of its carbon atom (89.1 ppm) was greater than that of the corresponding carbon atom of the R_S diastereomer (86.1 ppm), which is in agreement with the method for assignment of sulfoxide configuration proposed by Khiar.[26]

Conclusions

The evidence presented here shows that the most stable configurations of glycosyl sulfoxides are those that can adopt conformations with the aglycone exo and the lone pair on sulfur anti to the C1–O5 bond, because of the n → σ* overlap possible in this orientation. For D-pyranosides, these are the S_S configurations of the α-anomers and the R_S configurations of the β-anomers. Equilibration studies by Crich et al.[23] are in agreement with the conclusions drawn here for glycosyl sulfoxides with substitutents at C2 equatorial but indicate that the configuration at C2 has a major effect on glycosyl sulfoxide conformer stability. Electronegative substituents in equatorial orientations at C2 destabilize the conformation with the sulfoxide oxygen atom anti by about 2.5 kcal mol^{-1}. The calculations indicate that n → σ* overlap and the preference for the endocyclic C–O dipole and the S–O to adopt antiparallel conformations have effects that are about equal in size in determining glycosyl sulfoxide conformations in the gas phase or nonpolar solvents. For the less stable but kinetically favoured R_S diastereomers of the β-anomers, anti conformers are comparable in stability to the exo conformers because of the n → σ* overlap possible if the sulfur lone pair is a p-type lone pair.

The method for assignment of glycosyl sulfoxide configurations by comparing the ^{13}C NMR chemical shifts of C1 for the two diastereomers proposed by Khiar[26] was supported by the chemical shifts calculated by the Gauge invariant atomic orbital (GIAO) method. However, the explanation advanced for the rule that C1 from the S_S sulfoxide is more shielded that that of the R_S sulfoxide, because of n → σ* overlap in the S_S sulfoxide, does not appear to be correct.

Experimental section

General methods

Melting points were determined with a Fisher-Johns melting point apparatus and are uncorrected. ^1H and ^{13}C NMR spectra were recorded at 300 K in 5 mm NMR tubes on Bruker NMR spectrometers (AC-250, AMX-400, or Avance-500) operating at 250.13, 400.13, or 500.13 MHz for proton spectra and 62.9, 100.08, or 125.77 MHz for carbon spectra, respectively, on solutions in chloroform-*d*, unless otherwise indicated. Chemical shifts are given in parts per million (ppm; ±0.01 ppm) relative to that of tetramethylsilane (TMS; 0.00 ppm) in the case of ^1H NMR spectra and to the central line of chloroform-*d* (δ 77.16) for the ^{13}C NMR spectra. All assignments were confirmed by COSY, HETCOR, HMQC, HSQC, or HMBC experiments. Exact masses measured using electron ionization (EI; 70 eV) were done on a CEC 21-110B mass spectrometer. Electrospray mass spectra were recorded on a Fisons Quattro mass spectrometer with a Quattro source (cone voltage, 55 V; flow rate, 5 μL/min; complexing agent, potassium acetate; solvent, 75:25 *v*/*v* acetonitrile/water). Optical rotations were determined with a Rudolph Instruments Digipol 781 automatic polarimeter or with a PerkinElmer model 141 polarimeter. Thin layer chromatography (TLC) was performed on aluminum-backed plates bearing 200 μm silica gel 60 F_{254} (Merck or Silicycle). The ratio of the solvents used in TLC and column chromatography was a volume ratio. Compounds were visualized by UV where applicable and (or) were located by spraying with a solution of 2% ceric sulfate in 1 mol/L sulfuric acid followed by heating on a hot plate until colour developed. Compounds were purified on silica gel (TLC standard grade, 230–400 mesh) by flash chromatography using specified eluents. Elemental analyses were performed by the Canadian Microanalytical Service, Delta, British Columbia.

Pyridine was dried by refluxing over calcium hydride followed by distillation and stored over molecular sieves. Amberlite IR-120 (H^+) resin was washed with a 10% hydrochloric acid solution and distilled water, and then dried under vacuum at 50 °C overnight. Ammonium cerium (IV) nitrate and sodium azide were ground to powders and dried in vacuuo for 2 days. Boron trifluoride diethyl etherate was distilled before use.

X-ray crystallography

Crystals for X-ray structural determinations were mounted on glass fibers. All measurements were made on a Rigaku AFC5R diffractometer equipped with graphite-monochromated Mo Kα radiation (**6**, **8R**, **8S**, and **9R**) or Cu Kα radiation (**18S**) and a rotating anode generator. Cell constants and an orientation matrix for data collection were obtained from a least-squares refinement using the setting angles of a minimum of 24 reflections (with the exception of **12R** where only 10 reflections were obtained). The data were collected at temperatures of 23 °C (**8S** and **18S**), –100 °C (**6** and **9R**), or –130 °C (**8R**) using the ω–2θ scan technique. The intensities of three representative reflections were measured after every 150 reflections; no decay corrections were applied. An empirical absorption correction[62] based on azimuthal scans of several reflections was applied for every structure except **9R**. The data were corrected for Lorentz and polarization effects. Data reduction was carried out using the TEXSAN software package.[63] The structures were solved by direct methods using SIR-92.[64,65] Full-matrix least-squares refinement was carried out on F^2 data using SHELXL-97.[66] Secondary extinction was refined for **18S**. In all cases, the non-hydrogen atoms were refined anisotropically. Hydrogen atoms were included but not refined. They were placed in geometrically calculated positions and allowed to ride on the heavy atom to which they were bonded with isotropic temperature factors (U_{iso}) equal to 1.2 times Ueq of the heavy atom (1.5 times Ueq for methyl hydrogens).

NMR experiments

Experiments were performed on 0.04 mol/L solutions in acetone-d_6 unless otherwise specified. NOESY spectra were recorded on the Bruker Avance 500 MHz NMR spectrometer using different mixing times. Spectra were processed with Bruker's XWIN-NMR package. The matrices were transformed to a final size of 8192 and 2048 points in F2 and F1 dimensions, respectively. The signal was multiplied by a shifted qsin bell window in both dimensions prior to Fourier transformation, then phase and baseline corrections on both dimensions were applied. The numbers of contour layers were set at 18. For compound **6**, spectra were recorded with a relaxation delay of 1 s with mixing times of 0.3, 0.5, 0.7, 1, and 1.5 s. For **8R**, spectra were recorded with a relaxation delay of 2.5 s and mixing times of 0.5, 0.7, 0.9, 1.1, and 1.3 s. For compound **9R**, spectra were recorded with a relaxation delay of 1 s and mixing times of 0.3, 0.5, 0.7, 1, and 1.5 s.

Relaxation times were determined for compounds **6** and **8R** by the inversion recovery method to set the relaxation delays for the 1D NOE experiments. The t1ir pulse program on the 500 MHz NMR spectrometer was used to acquire data and the proc_t1 program was used to process data. The results are shown in Table S4 in the Supplementary data. Based on these results, the delay time used for 1D gradient NOE experiments was set at 10 s. The selnogp pulse sequence was used for 1D gradient NOE experiments. For compounds **6**, **8R**, and **8S**, the signals of H–SPo were irradiated and mixing times of of 0.3, 0.5, 0.75, 0.9, 1, 1.1, and 1.25 s; 0.3, 0.9, 1.25, 1.5, 1.75, and 2.25 s; and 0.5, 0.75, 1, 1.25, 1.5, 1.75, 2, 2.25, 2.5, and 3 s, respectively, were used.

The distance between ortho phenyl protons (r = 2.8 Å) was used as the reference distance to calculate internuclear distances using the equation

$$r_{IS} = r_{ref}\left(\frac{NOE_{ref}}{NOE_{IS}}\right)^{1/6}$$

Computational methods

Most geometry optimizations were carried out at the B3LYP hybrid density functional in conjunction with the B3LYP/6–31G(d) basis set using the Gaussian 03 suite of programs.[52] The B3LYP functional is a combination of Becke's three-parameter hybrid exchange functional and Lee–Yang–Parr correlational functional.[53,54] Harmonic vibrational frequencies and zero-point vibrational energies (ZPVEs) were obtained at the same level of theory. Relative energies were obtained by performing single-point calculations at the B3LYP level of theory with the 6–311G+(d,p) basis set using the above optimized geometries and by including the zero-point vibrational energy, i.e., B3LYP/6–311G+(d,p)//B3LYP/6–31G(d) + ZPVE. Compounds **12**–**15** were also optimized at the 6–311G+(d,p) level of theory. The GIAO method was used for ^{13}C shielding calculations using the 6–311+G(d,p) basis set.

Synthetic procedures

Phenyl 2-azido-2-deoxy-1-thio-α-D-galactopyranoside (1) and phenyl 2-azido-2-deoxy-1-thio-β-D-galactopyranoside (2)

Freshly distilled boron trifluoride diethyl etherate (19 mL, 151.3 mmol, 5.6 equiv) was added dropwise to a stirred clear colorless solution of thiophenol (14 mL, 136.0 mmol, 5 equiv) and 2-azido-2-deoxy-1,3,4,6-tetra-*O*-acetyl-α-D-galactopyranoside[37] (10.07 g, 27.0 mmol) in chloroform (175 mL) at 0 °C. The reaction mixture was stirred at room temperature (RT) for 24 h. The clear orange solution was washed with saturated sodium bicarbonate aqueous solution (3 × 30 mL) and distilled water (3 × 30 mL), dried (anhydrous sodium sulphate), filtered, and concentrated to give a yellow syrup, phenyl 3,4,6-tetra-*O*-acetyl-2-azido-2-deoxy-1-thio-*O*-acetyl-D-galactopyranoside.

The yellow syrup was taken up in methanol (100 mL) and a solution of sodium methoxide in methanol (100 mL, 1.2 mol/L) was added. The basic solution was stirred for 1 h, neutralized by Amberlite IR-120 (H^+), filtered, and concentrated to a yellow syrup, phenyl 2-azido-2-deoxy-1-thio-D-galactopyranoside. The α–β mixture was separated by column chromatography (ethyl acetate – hexanes, 10:1). The pure anomers were crystallized from ethanol–hexanes.

α-Isomer (1)

Colorless needles; yield: 3.21 g (40%); mp 130.0–133.0 °C. $[\alpha]_D^{25}$ +252.2° (*c* 1.3, ethanol). R_f = 0.34. ^1H NMR (acetone-d_6) δ: 7.58–7.29 (m, 5H, Ph), 5.67 (d, 1H, $J_{1,2}$ = 5.4 Hz, H-1), 4.47 (d, 1H, $J_{3,OH}$ = 7.1 Hz, OH-3), 4.31 (t, 1H, H-5), 4.17 (dd, 1H, $J_{2,3}$ = 10.5 Hz, H-2), 4.15 (d, 1H, $J_{4,OH}$ = 3.7 Hz, OH-4), 4.09 (ddd, 1H, $J_{3,4}$ = 3.4 Hz, $J_{4,5}$ = 1.3 Hz, H-4), 3.84 (ddd, 1H, H-3), 3.79–3.69 (m, 3H, 2 × H-6, OH-6). ^{13}C NMR (acetone-d_6) δ: 135.4, 133.1, 129.9, 128.2 (Ph), 88.8 (C-1), 73.2 (C-5), 71.1 (C-3), 70.0 (C-4), 62.1 (C-6), 62.0 (C-2). HR-MS (EI, *m/z*) calcd. for $[C_{12}H_{15}N_3O_4S]^+$: 297.0783; found: 297.0793.

β-Isomer (2)

Colorless needles; yield: 3.09 g (39%); mp 149.0–149.5 °C. $[\alpha]_D^{25}$ +24.0° (*c* 0.3, ethanol). R_f = 0.26. ^1H NMR (acetone-d_6) δ: 7.58–7.29 (m, 5H, aromatic protons), 4.60 (d, 1H, $J_{1,2}$ = 10.0 Hz, H-1), 4.53 (d, 1H, $J_{3,OH}$ = 7.3 Hz, OH-3), 4.05 (d, 1H, $J_{4,OH}$ = 4.1 Hz, OH-4), 3.98 (dd, 1H, $J_{3,4}$ = 3.2 Hz, $J_{4,5}$ < 1 Hz, H-4), 3.90 (dd, 1H, $J_{6,OH}$ = 6.8 Hz, $J_{6',OH}$ = 6.6 Hz, OH-6), 3.79 (m, 2H, H6 and H6′), 3.68 (ddd, 1H, $J_{2,3}$ = 10.5 Hz, H –3), 3.65 (dd, 1H, $J_{5,6}$ = 6.6 Hz, $J_{5,6'}$ = 3.9 Hz, H-5), 3.57 (dd, 1H, H-2). ^{13}C NMR (acetone-d_6) δ: 132.5, 129.8, 128.3 (Ph), 86.8 (C-1), 80.1 (C-5), 74.9 (C-3), 69.3 (C-4), 64.2 (C-2), 62.2 (C-6). HR-MS (EI, *m/z*) calcd. for $[C_{12}H_{15}N_3O_4S]^+$: 297.0783; found: 297.0794.

Phenyl 2-azido-4,6-O-benzylidene-2-deoxy-1-thio-α-D-galactopyranoside (3)

A solution of compound **1** (2.98 g, 10.0 mmol), *p*-methoxybenzoic acid (0.10 g), and benzaldehyde (5 mL, 50.0 mmol, 5 equiv) in DMF–benzene (100 mL, 3:2 *v/v*) was refluxed in an apparatus for the azeotropic removal of water for 15 h. After TLC showed complete disappearance of the starting material, the reaction mixture was cooled to RT, neutralized with anhydrous potassium carbonate (1.00 g), filtered, and concentrated to yield an orange syrup, which was purified by flash column chromatography. Crystallization from ethanol–hexanes gave the title compound (**3**) as colorless needles; yield: 3.50 g (91%); mp 114.5–115.5 °C. $[\alpha]_D^{23}$ +157.7° (*c* 0.8, $CHCl_3$); lit. value[38] $[\alpha]_D$ +134.9° (*c* 0.5, $CHCl_3$). R_f = 0.35 (ethyl acetate – hexanes 1:3). ^1H NMR δ: 7.48–7.28 (m, 10H, Ph), 5.76 (d, 1H, $J_{1,2}$ = 5.3 Hz, H-1), 5.62 (s, 1H, C*H*Ph), 4.34 (dd, 1H, $J_{3,4}$ = 3.4 Hz, $J_{4,5}$ = 0.8 Hz, H-4), 4.27 (bs, 1H, H-5), 4.26 (dd, 1H, $J_{5,6a}$ = 1.6 Hz, $J_{6a,6e}$ = 12.5 Hz, H-6a), 4.21 (dd, 1H, $J_{2,3}$ = 10.5 Hz, H-2), 4.16 (dd, 1H, $J_{5,6e}$ = 1.5 Hz, H-6e), 4.03 (ddd, 1H, $J_{3,OH}$ = 10.4 Hz, H –3), 2.54 (d, 1H, 3-OH). ^{13}C NMR δ: 137.2, 137.7, 131.2, 129.5, 129.2, 128.4, 127.5, 126.2 (Ph), 101.4 (*C*HPh), 87.4 (C-1), 75.2 (C-4), 69.6 (C-3), 69.2 (C-6), 63.7 (C-5), 61.5 (C-2). HR-MS (EI, *m/z*) calcd. for $[C_{19}H_{19}N_3O_4S]^+$: 385.1096; found: 385.1107.

Phenyl 2-azido-4,6-O-benzylidene-2-deoxy-1-thio-β-D-galactopyranoside (4)

Following the same procedure as in the preparation of compound **3**, compound **4** (3.21 g, 10.8 mmol) gave the title compound as colorless needles; yield: 3.70 g (89%); mp 79.0–80.0 °C. $[\alpha]_D^{20}$ –23.0° (*c* 0.5, $CHCl_3$). R_f = 0.4 (ethyl acetate – hexanes, 1:1). ^1H NMR (500 MHz) δ: 7.79–7.33 (m, 10H, Ph), 5.58 (s, 1H, C*H*Ph), 4.47 (d, 1H, $J_{1,2}$ = 9.8 Hz, H-1), 4.46 (dd, 1H, $J_{5,6a}$ = 1.2 Hz, H-6a), 4.24 (d, 1H, $J_{3,4}$ = 3.5 Hz, 1H, H-4), 4.09 (dd, 1H, $J_{5,6e}$ = 1.4 Hz, $J_{6a,6e}$ = 12.5 Hz, H-6e), 3.70 (ddd, 1H, $J_{2,3}$ = 9.7 Hz, $J_{OH,3}$ = 9.8 Hz, H-3), 3.58 (dd, 1H, H-2), 3.57 (bs, 1H, H-5), 2.55 (d, 1H, 3-OH). ^1H NMR (acetone-*d*6, 500 MHz) δ: 7.74–7.31 (m, 10H, Ph), 5.68 (s, C*H*Ph), 4.68 (d, 1H, $J_{1,2}$ = 9.9 Hz, H-1), 4.58 (d, 1H, $J_{OH,3}$ = 8.8 Hz, 3-OH), 4.33 (d, 1H, $J_{3,4}$ = 2.7 Hz, 1H, H-4), 4.27 (dd, 1H, $J_{5,6a}$ = 1.4 Hz, $J_{6a,6e}$ = 12.2 Hz, H-6a), 4.18 (dd, 1H, $J_{5,6e}$ = 1.6 Hz, H-6e), 3.81 (ddd, 1H, $J_{2,3}$ = 9.7 Hz, H-3), 3.79 (bs, 1H, H-5), 3.69 (d, 1H, H-2). ^{13}C NMR δ: 137.4, 134.3, 130.4, 129.5, 129.0, 128.5, 128.3, 126.5 (Ph), 101.5 (*C*HPh), 85.2 (C-1), 74.5 (C-4), 73.3 (C-3), 69.9 (C-5), 69.3 (C-6), 62.2 (C-2). ^{13}C NMR (acetone-d_6) δ: 139.0, 133.1, 132.1, 129.0, 128.8, 128.0, 127.9, 126.7 (Ph), 100.9 (*C*HPh), 84.9 (C-1), 75.5 (C-4),

73.0 (C-3), 70.1 (C-5), 69.1 (C-6), 62.5 (C-2). HR-MS (EI, *m*/*z*) calcd. for $[C_{19}H_{19}N_3O_4S]^+$: 385.1096; found: 385.1088.

*Phenyl 2-azido-2-deoxy-4,6-***O***-(*p*-methoxybenzylidene)-1-thio-α-D-galactopyranoside (5)*

A solution of compound **1** (0.97 g, 3.26 mmol), *p*-anisaldehyde (3.2 mL), and *p*-toluenesulfonic acid (80.0 mg) in DMF–benzene (65 mL, 3:2) was refluxed for 45 h in an apparatus for the azeotropic removal of water. After TLC showed that the starting material had disappeared, the reaction mixture was cooled to RT, neutralized by anhydrous potassium carbonate (1.00 g), filtered, and concentrated to a brown syrup. Purification by column chromatography (ethyl acetate – hexanes, 1:3) gave a colorless solid that crystallized from ethanol–hexanes as colorless needles; yield: 1.18 g (87%); mp 133.5–134.0 °C. $[\alpha]_D^{23}$ +89.1° (*c* 0.5, chloroform). R_f = 0.43 (ethyl acetate – hexanes, 1:2). ^{1}H NMR δ: 7.48–7.26 (m, 8H, Ph), 6.91 (d, 1H, Ph), 5.76 (d, 1H, $J_{1,2}$ = 5.3 Hz, H-1), 5.58 (s, 1H, C*H*Ph), 4.32 (bd, 1H, $J_{3,4}$ = 3.5 Hz, H-4), 4.26 (bs, 1H, H-5), 4.24 (bd, 1H, H-6a), 4.20 (dd, 1H, $J_{2,3}$ = 10.6 Hz, H-2), 4.12 (dd, 1H, $J_{5,6a}$ = 1.5 Hz, $J_{6a,6b}$ = 12.3 Hz, H-6b), 4.03 (ddd, 1H, $J_{3,OH}$ = 10.4 Hz, H-3), 2.55 (d, 1H, 3-OH). ^{13}C NMR δ: 160.5, 133.7, 129.7 (tertiary aromatic carbons), 131.2, 129.2, 127.7, 127.5, 113.7 (Ph), 101.4 (*C*HPh), 87.3 (C-1), 75.1 (C-4), 69.6 (C-3), 69.2 (C-6), 63.7 (C-5), 61.5 (C-2), 55.4 (OCH_3).

*Phenyl 3-***O***-acetyl-2-azido-4,6-***O***-benzylidene-2-deoxy-1-thio-α-D-galactopyranoside (6)*

Acetic anhydride (1.5 mL, 97%, 15.0 mmol, 5 equiv) was added to a solution of compound **3** (1.15 g, 2.98 mmol) in dry pyridine (10 mL). The reaction mixture was stirred at RT for 24 h, and then concentrated under vacuum to give a colorless syrup. The syrup was dissolved in chloroform (15 mL). The solution was washed with saturated sodium bicarbonate aqueous solution (3 mL) and distilled water (3 mL), dried over sodium sulphate anhydrous, filtered, and concentrated to yield a colorless syrup. The syrup was crystallized from diethyl ether to give a colorless solid and recrystalized from ethanol–chloroform as colorless needles; yield: 1.20 g (94%); mp 154.5–155.5 °C. [α] +198.9° (*c* 0.6, $CHCl_3$). ^{1}H NMR δ: 7.50–7.24 (m, 10H, Ph), 5.81 (d, 1H, $J_{1,2}$ = 5.3 Hz, H-1), 5.56 (s, 1H, C*H*Ph), 5.13 (dd, 1H, $J_{2,3}$ = 11.0 Hz, $J_{3,4}$ = 3.4 Hz, H-3), 4.57 (dd, 1H, H-2), 4.53 (d, 1H, H-4), 4.26 (bs, 1H, H-5), 4.22 (dd, 1H, $J_{5,6a}$ = 1.4 Hz, $J_{6a,6e}$ = 12.6 Hz, H-6a), 4.09 (dd, 1H, $J_{5,6e}$ = 1.7 Hz, H-6e), 2.16 (s, 3H, $COCH_3$). ^{13}C NMR (acetone-d_6) δ: 170.6 (C=O), 139.5, 134.5, 132.9, 129.3, 128.9, 128.5, 127.3 (Ph), 101.4 (*C*HPh), 88.3 (C-1), 74.2 (C-4), 71.5 (C-3), 69.6 (C-6), 64.7 (C-5), 59.0 (C-2), 20.8 ($CO*C*H_3$). HR-MS (EI, *m*/*z*) calcd. for $[C_{21}H_{21}N_3O_5S]^+$: 427.1202; found: 427.1202.

*Phenyl 3-***O***-acetyl-2-azido-2-deoxy-4,6-***O***-(*p*-methoxybenzylidene)-1-thio-α-D-galactopyranoside (7)*

Acetic anhydride (2 mL, 97%, 20.0 mmol) was added to a solution of compound **5** (1.18 g, 2.84 mmol) in dry pyridine (10 mL) and the reaction mixture was stirred at RT for 16 h, and was then concentrated under vacuum to give a orange syrup that was azeotroped with toluene (3 × 4 mL) to give a yellow solid that on crystallization from ethanol, appeared as colorless needles; yield: 1.26 g (97%); mp 138.5–140.0 °C. [α] +206.2° (*c* 0.6, $CHCl_3$). R_f = 0.33 (ethyl acetate – hexanes, 1:3). ^{1}H NMR δ: 7.50–6.88 (m, 9H, Ph), 5.80 (d, 1H, $J_{1,2}$ = 5.5 Hz, H-1), 5.51 (s, 1H, C*H*Ph), 5.12 (dd, 1H, $J_{2,3}$ = 11.0 Hz, $J_{3,4}$ = 3.1 Hz, H –3), 4.57 (dd, 1H, H-2), 4.50 (d, 1H, H-4), 4.24 (bs, 1H, H-5), 4.20 (dd, 1H, $J_{5,6a}$ = 1.4 Hz, $J_{6a,6b}$ = 12.8 Hz, H-6a), 4.07 (dd, 1H, $J_{5,6b}$ = 1.5 Hz, H-6b), 3.81 (s, 3H, OCH_3), 2.16 (s, 3H, $COCH_3$). ^{13}C NMR δ: 170.3 (C=O), 160.2, 133.4, 130.0 (tertiary aromatic carbons), 131.3, 129.1, 127.5, 113.6 (Ph), 100.9 (*C*HPh), 87.3 (C-1), 73.1 (C-4), 71.4 (C-3), 69.1 (C-6), 63.4 (C-5), 57.8 (C-2), 55.3 (OCH_3), 20.95 ($CO*C*H_3$).

*(R_S) Phenyl 2-azido-4,6-***O***-benzylidene-2-deoxy-1-thio-α-D-galactopyranoside* **S***-oxide (8R) and (S_S) phenyl 2-azido-4,6-***O***-benzylidene-2-deoxy-1-thio-α-D-galactopyranoside* **S***-oxide (8S)*

A solution of *m*-chloroperbenzoic acid (0.22 g, 77%, 1.02 mmol, 1.1 equiv) in dichloromethane (2 mL) was added to a mixture of compound **6** (0.40 g, 0.93 mmol) and sodium bicarbonate (0.10 g, 1.21 mmol, 1.3 equiv) in dichloromethane (8 mL) at –76 °C. The reaction mixture was stirred at –76 °C for 16 h. The reaction mixture was allowed to warm to RT and then diluted with dichloromethane (10 mL). The mixture was washed with 20% sodium thiosulfate (5 mL), saturated aqueous sodium bicarbonate solution (5 mL), and distilled water (5 mL), and then dried (sodium sulphate), filtered, and concentrated to give a colorless solid. Fractionation by column chromatography (ethyl acetate – hexanes, 1:2) yielded three compounds.

Compound **8R** was crystallized from ethanol–chloroform; yield: 247.5 mg (60%); mp 191.5–192.5 °C. $[\alpha]_D^{22}$ +34.6° (*c* 0.4, $CHCl_3$). R_f = 0.20. ^{1}H NMR (500 MHz) δ: 7.54 (m, 2H, H*o*-SPh), 7.45 (m, 3H, H*p*-SPh and H*m*-SPh), 7.36 (m, 5H, H*o*-CH*Ph*, H*m*-CH*Ph*, and H*p*-CH*Ph*), 5.78 (dd, 1H, $J_{2,3}$ = 10.8 Hz, $J_{3,4}$ = 3.4 Hz, H-3), 5.53 (s, 1H, C*H*Ph), 4.95 (s, 1H, $J_{1,2}$ = 5.7 Hz, H-1), 4.65 (dd, 1H, H-2), 4.62 (d, 1H, H-4), 4.11 (bs, 1H, H-5), 4.14 (dd, 1H, $J_{5,6e}$ = 1.5 Hz, H-6e), 4.02 (dd, 1H, $J_{5,6a}$ = 2.2 Hz, $J_{6a,6e}$ = 12.3 Hz, H-6a), 2.16 (s, 3H, $COCH_3$). ^{1}H NMR (acetone-d_6, 500 MHz) δ: 7.86 (d, 2H, H*o*-SPh), 7.65 (t, 2H, H*m*-SPh), 7.60 (t, 2H, H*p*-SPh), 7.51 (m, 2H, H*o*-CH*Ph*), 7.39 (m, 3H, H*m*-CH*Ph* and H*p*-CH*Ph*), 5.85 (dd, 1H, $J_{2,3}$ = 11.0 Hz, $J_{3,4}$ = 3.5 Hz, H-3), 5.69 (s, 1H, C*H*Ph), 5.15 (d, 1H, $J_{1,2}$ = 6.6 Hz, H-1), 4.78 (dd, 1H, H-2), 4.66 (d, 1H, H-4), 4.32 (bs, 1H, H-5), 4.21 (dd, 1H, $J_{5,6a}$ = 1.5 Hz, $J_{6a,6e}$ = 12.7 Hz, H-6a), 4.09 (dd, 1H, $J_{5,6e}$ = 1.5 Hz, H-6a), 2.12 (s, 3H, $COCH_3$). ^{1}H NMR (CD_2Cl_2, 500 MHz) δ: 7.77 (m, 2H, H*o*-SPh), 7.63 (m, 2H, H*m*-SPh), 7.61 (t, 2H, H*p*-SPh), 7.50 (m, 2H, H*o*-CH*Ph*), 7.43 (m, 3H, H*m*-CH*Ph* and H*p*-CH*Ph*), 5.86 (dd, 1H, $J_{2,3}$ = 10.8 Hz, $J_{3,4}$ = 3.5 Hz, H-3), 5.58 (s, 1H, C*H*Ph), 5.01 (d, 1H, $J_{1,2}$ = 5.6 Hz, H-1), 4.67 (dd, 1H, H-2), 4.61 (d, 1H, H-4), 4.20 (bs, 1H, H-5), 4.15 (dd, 1H, $J_{5,6a}$ = 1.6 Hz, $J_{6a,6e}$ = 12.8 Hz, H-6a), 4.07 (dd, 1H, $J_{5,6e}$ = 1.6 Hz, H-6a), 2.19 (s, 3H, $COCH_3$). ^{1}H NMR (CD_3CN, 500 MHz) δ: 7.80 (m, 2H, H*o*-SPh), 7.63 (m, 3H, H*m*-SPh and H*p*-SPh), 7.48 (m, 2H, H*o*-CH*Ph*), 7.42 (m, 3H, H*m*-CH*Ph* and H*p*-CH*Ph*), 5.78 (dd, 1H, $J_{2,3}$ = 11.0 Hz, $J_{3,4}$ = 3.4 Hz, H-3), 5.61 (s, 1H, C*H*Ph), 5.07 (d, 1H, $J_{1,2}$ = 5.6 Hz, H-1), 4.70 (dd, 1H, H-2),

4.54 (d, 1H, H-4), 4.14 (bs, 1H, H-5), 4.05 (dd, 1H, $J_{5,6a}$ = 1.4 Hz, $J_{6a,6e}$ = 12.9 Hz, H-6a), 3.95 (dd, 1H, $J_{5,6e}$ = 1.4 Hz, H-6a), 2.17 (s, 3H, $COCH_3$). ^{13}C NMR δ: 170.1 (C=O), 141.3, 137.2, 131.3, 129.2, 129.2, 128.3, 126.0, 124.8 (Ph), 100.7 (*C*HPh), 96.3 (C-1), 72.7 (C-4), 70.2 (C-3), 68.9 (C-6), 67.6 (C-5), 57.9 (C-2), 20.9 ($COCH_3$). HR-MS (EI, *m*/*z*) calcd. for $[C_{21}H_{21}N_3O_6S - N_2]^+$: 415.1089; found: 415.1096.

Compound **8S** was crystallized from ethanol–chloroform; yield: 82.1 mg (20%); mp 197.5–198.5 °C. $[\alpha]_D$ +367.7° (*c* 0.6, $CHCl_3$). R_f = 0.45. ^1H NMR (500 MHz) δ: 7.63 (d, 2H, H*o*-SPh), 7.55 (t, 1H, H*p*-SPh), 7.52 (t, 2H, H*m*-SPh), 7.43 (m, 2H, H*o*-CH*Ph*), 7.35 (m, 3H, H*m*-CH*Ph* and H*p*-CH*Ph*), 5.94 (dd, 1H, $J_{2,3}$ = 10.9 Hz, $J_{3,4}$ = 3.3 Hz, H-3), 5.49 (s, 1H, C*H*Ph), 4.90 (s, 1H, H-5), 4.76 (dd, 1H, $J_{1,2}$ = 6.6 Hz, H-2), 4.61 (d, 1H, H-4), 4.56 (d, 1H, H-1), 4.01 (dd, 1H, $J_{5,6e}$ = 1.4 Hz, $J_{6a,6e}$ = 12.9 Hz, H-6e), 3.90 (dd, 1H, $J_{5,6a}$ = 1.3 Hz, H-6a), 2.12 (s, 3H, $COCH_3$). ^1H NMR (acetone-d_6, 500 MHz) δ: 7.78 (d, 2H, H*o*-SPh), 7.67 (t, 2H, H*m*-SPh), 7.62 (t, 2H, H*p*-SPh), 7.48 (m, 2H, H*o*-CH*Ph*), 7.37 (t, 3H, H*m*-CH*Ph* and H*p*-CH*Ph*), 6.02 (m, 1H, H-3), 5.64 (s, 1H, C*H*Ph), 4.92–4.89 (m, 3H, H-1, H-2, H-5), 4.63 (d, 1H, $J_{3,4}$ = 2.5 Hz, H-4), 4.07 (dd, 1H, $J_{5,6e}$ = 1.3 Hz, $J_{6a,6e}$ = 12.8 Hz, H-6e), 3.85 (dd, 1H, $J_{5,6a}$ = 1.4 Hz, H-6a), 2.12 (s, 3H $COCH_3$). ^{13}C NMR δ: 170.0 (C=O), 140.5, 137.3, 131.1, 129.2, 129.1, 128.2, 126.0, 124.7 (Ph), 100.7 (*C*HPh), 92.5 (C-1), 73.0 (C-4), 71.2 (C-3), 68.8 (C-4), 68.7 (C-6), 57.3 (C-2), 21.0 ($COCH_3$). ^{13}C NMR (acetone-d_6) δ: 169.6 (C=O), 141.4, 138.7, 130.9, 129.8, 128.8, 128.0, 126.4, 125.0 (Ph), 100.4 (*C*HPh), 92.4 (C-1), 73.2 (C-4), 70.4 (C-3), 69.1 (C-5), 68.4 (C-6), 58.2 (C-2), 20.1 ($COCH_3$). MS (ESI, *m*/*z*) calcd. for $[C_{21}H_{21}N_3O_6S + Na]^+$: 466.0; found: 466.0. HR-MS (EI, *m*/*z*) calcd. for $[C_{21}H_{21}N_3O_6S - C_6H_5OS]^+$: 318.1090; found: 318.1098.

The third fraction was phenyl 2-azido-4,6-*O*-benzylidene-2-deoxy-1-thio-α-D-galactopyranoside dioxide; yield: 46.8 mg (11%); mp 183.0–184.0 °C. $[\alpha]_D^{23}$ +131.4° (*c* 0.4, $CHCl_3$). R_f = 0.42. ^1H NMR (acetone-d_6, 500 MHz) δ: 8.04 (d, 2H, *o*-SPh), 7.82 (t, 1H, *p*-SPh), 7.73 (t, 2H, *m*-SPh), 7.41 (d, 2H, *J* = 7.1 Hz, *o*-Ph), 6.92 (d, 2H, *m*-Ph), 5.85 (dd, 1H, $J_{2,3}$ = 11.3 Hz, $J_{3,4}$ = 3.4 Hz, H-3), 5.63 (s, 1H, C*H*Ph), 5.55 (d, 1H, $J_{1,2}$ = 6.0 Hz, H-1), 4.83 (dd, 1H, H-2), 4.64 (bs, 1H, H-4), 4.41 (bs, 1H, H-5), 4.16 (d, 1H, $J_{6a,6e}$ = 12.4 Hz, H-6a), 3.89 (d, 1H, H-6e), 3.82 (s, 3H, OCH_3), 2.83 (s, 3H, $COCH_3$). ^1H NMR (500 MHz) δ: 7.92 (d, 2H, *o*-SPh), 7.68 (t, 1H, *p*-SPh), 7.58 (t, 2H, *m*-SPh), 7.44–7.35 (m, 4H, Ph), 5.87 (dd, 1H, $J_{2,3}$ = 11.1 Hz, $J_{3,4}$ = 3.4 Hz, H-3), 5.52 (s, 1H, C*H*Ph), 5.13 (d, 1H, $J_{1,2}$ = 6.3 Hz, H-1), 4.66 (dd, 1H, H-2), 4.64 (bs, 1H, H-4), 4.35 (bs, 1H, H-5), 4.06 (d, 1H, $J_{5,6a}$ = 1.3 Hz, $J_{6a,6e}$ = 12.8 Hz, H-6a), 3.99 (d, 1H, $J_{5,6e}$ = 1.2 Hz, H-6e), 3.82 (s, 3H, OCH_3), 2.17 (s, 3H, $COCH_3$). ^{13}C NMR δ: 170.1 (C=O), 138.8, 137.3, 134.4, 129.4, 128.9, 128.4, 126.1 (Ph), 100.9 (*C*HPh), 89.9 (C-1), 72.7 (C-4), 69.9 (C-3), 68.9 (C-6), 67.1 (C-5), 56.3 (C-2), 21.1 ($COCH_3$). MS (ESI, *m*/*z*) calcd. for $[C_{21}H_{21}N_3O_7S + Na]^+$: 482.0; found: 482.0. HR-MS (EI, *m*/*z*) calcd. for $[C_{21}H_{21}N_3O_7S - C_6H_5O_2S]^+$: 318.1090; found: 318.1092.

(R_S) Phenyl 3-O-acetyl-2-azido-2-deoxy-4,6-O-(p-methoxybenzylidene)-1-thio-α-D-galactopyranoside S-*oxide (9R) and (S_S) phenyl 3-O-acetyl-2-azido-2-deoxy-4,6-O-(p-methoxybenzylidene)-1-thio-α-D-galactopyranoside* S-*oxide (9S)*

Following the same procedure as for compound **6**, compounds **9R** and **9S** were obtained from compound **8** (0.30 g), *m*-chloroperbenzoic acid (0.13 g), and sodium hydrogen carbonate (0.07 g), followed by separation by column chromatography on silica gel using the same solvent system.

Compound **9R** was crystallized from ethanol–chloroform to give colorless needles; yield: 0.22 g (70%); mp 161.5–163.0 °C. $[\alpha]_D^{23}$ +44.4° (*c* 0.3, chloroform). R_f = 0.17 (ethyl acetate – hexanes, 1:2). ^1H NMR δ: 7.71–6.89 (m, 9H, aromatic protons), 5.76 (dd, 1H, $J_{2,3}$ = 11.0 Hz, $J_{3,4}$ = 3.7 Hz, H-3), 5.48 (s, 1H, C*H*Ph), 4.95 (d, 1H, $J_{1,2}$ = 5.5 Hz, H-1), 4.64 (dd, 1H, H-2), 4.60 (bd, 1H, $J_{4,5}$ < 1 Hz, H-4), 4.08 (bs, 1H, H-5), 4.10, 3.98 (2H, AB part of ABX pattern, $J_{5,6a}$ = 1.2 Hz, $J_{5,6b}$ = 2.4 Hz, $J_{6a,6b}$ = 12.5 Hz, H-6a, H-6b), 3.80 (s, 3H, OCH_3), 2.16 (s, 3H, $COCH_3$). ^{13}C NMR δ: 170.2 (C=O), 160.3, 141.4, 131.4, 129.7, 129.2, 127.4, 124.9, 113.7 (Ph), 100.8 (*C*HPh), 96.3 (C-1), 72.7 (C-4), 70.4 (C-3), 68.9 (C-6), 67.6 (C-5), 57.9 (C-2), 55.3 (OCH_3), 20.9 (CO*C*H3). HR-MS (EI, *m*/*z*) calcd. for $[C_{22}H_{23}N_3O_7S - C_6H_5OS]^+$: 348.1195; found: 348.1188.

Compound **9S** was crystallized from ethanol–chloroform to give colorless needles; yield: 56 mg (19%); mp 224.0–224.5 °C. $[\alpha]$ +153.8° (*c* 0.3, chloroform). R_f = 0.30 (ethyl acetate – hexanes, 1:2). ^1H NMR δ: 7.65–7.54 (m, 5H, PhH), 7.36, 6.87 (2d, 4H, PhH), 5.86 (dd, 1H, $J_{2,3}$ = 11.0 Hz, $J_{3,4}$ = 3.4 Hz, H-3), 5.47 (s, 1H, C*H*Ph), 5.14 (d, 1H, $J_{1,2}$ = 6.3 Hz, H-1), 4.65 (dd, 1H, H-2), 4.61 (bd, 1H, $J_{4,5}$ < 1 Hz, H-4), 4.43 (bs, 1H, H-5), 4.02, 3.98 (2H, AB part of ABX pattern, $J_{5,6a}$ = 1.5 Hz, $J_{5,6b}$ = 1.6 Hz, $J_{6a,6b}$ = 12.8 Hz, H-6a, H-6b), 3.79 (s, 3H, OCH_3), 2.16 (s, 3H, $COCH_3$). ^{13}C NMR δ: 170.3 (C=O), 160.4, 138.7, 134.4, 129.8, 129.4, 128.9, 127.6, 113.8 (Ph), 100.9 (*C*HPh), 89.9 (C-1), 72.7 (C-4), 69.9 (C-3), 68.8 (C-6), 67.1 (C-5), 56.2 (C-2), 55.5 (OCH_3), 21.1 ($COCH_3$).

Phenyl 3,4,6-tri-O-acetyl-2-deoxy-2-phthalimido-1-thio-β-D-glucopyranoside (17)

1,3,4,6-Tetra-*O*-acetyl-2-deoxy-2-phthalimido-β-D-glucopyranose[45–47] (72.2 g, 0.15 mol) was treated with thiophenol and boron trifluoride etherate to give the title compound as a solid that was crystallized from 15% ethyl acetate in hexanes; yield: 64.4 g (81%); mp 140–141 °C, lit.value[48] mp 145–146 °C. $[\alpha]_D^{25}$ 49.4° (*c* 0.88, chloroform); lit. value[48] $[\alpha]_D^{25}$ 53.0°.

(S_S) Phenyl 3,4,6-tri-O-acetyl-2-deoxy-2-phthalimido-1-thio-β-D-glucopyranoside S-*oxide (18S)*

A solution of *m*-chloroperbenzoic acid (0.60 g, 70%, 3.4 mmol, 1.0 equiv) in dry dichloromethane (7 mL) was added to a precooled solution of compound **17** (1.22 g, 2.31 mmol) in dichloromethane (18 mL) at –78 °C. The reaction mixture was stirred at –78 °C for 26 h and then allowed to warm to RT over 12 h. The mixture was washed with saturated sodium bicarbonate solutions (3 × 25 mL) and water (25 mL), and then dried (sodium sulphate), fil-

tered, and concentrated to give a bright yellowish solid. Separation by flash column chromatography (ethyl acetate – hexanes, 1:1) gave the starting material (0.22 g) and colorless crystals of the product (0.95 g, 92% based on starting material consumed). Further fractionation using flash column chromatography (5% acetone in chloroform) gave **18S** as fluffy crystals that were recrystallized from 1% ethanol in hexanes to give clear colorless needles; mp 124–126 °C. $[\alpha]_D^{25}$ +113° (*c* 0.6, chloroform). R_f = 0.68 (5% acetone in chloroform). ^{1}H NMR (400 MHz) δ: 7.68 (bd s, 2H, Phth-H), 7.84–7.60 (very bd s, 2H, Phth-H), 7.49 (d, 2H, J = 7.5 Hz, *o*-Ar H), 7.21 (t, 2H, J = 7.5 Hz, *m*-Ar H), 7.13 (t, 1H, J = 7.3 Hz, *p*-Ar H), 5.77 (t, 1H, $J_{2,3} = J_{3,4}$ = 9.7 Hz, H-3), 5.40 (d, 1H, $J_{1,2}$ = 10.1 Hz, H-1), 5.16 (t, 1H, $J_{3,4} = J_{4,5}$ = 9.7 Hz, H-4), 4.89 (t, 1H, H-2), 4.20 and 4.28 (AB part of ABX pattern, 2H, $J_{6a,6b}$ = 12.3 Hz, $J_{5,6a} = J_{5,6b}$ = 4.9 Hz, 2 H-6), 3.91 (m, 1H, H-5), 2.09, 2.05, 1.85 (3s, 9H, 3 Ac). ^{13}C NMR (100 MHz) δ: 170.1, 169.8, 168.9 (3 Ac C=O), 167.6 (2 phth C=O), 138.8, 130.2, 128.4, 123.0 (S-Ph C), 133.9, 130.8, 123.9 (Phth C), 89.1 (C-1), 76.0 (C-5), 71.1 (C-3), 67.6 (C-4), 61.4 (C-6), 47.4 (C-2), 20.4, 20.2, 20.0 (Ac Me).

The second fraction was obtained as colorless fluffy crystals that decomposed on standing or on attempted recrystallization, R_f = 0.54 (5% acetone in chloroform). ^{1}H NMR (400 MHz) δ: 7.90 (half of AA′BB′ pattern, 2H, *o*-Phth-H), 7.90 (d, 2H, *o*-Ph H), 7.76 (half of AA′BB′ pattern, 2H, Phth-H), 7.70 (t, 1H, J = 7.5 Hz, *p*-Ar H), 7.58 (t, 2H, J = 7.7 Hz, *m*-Ar H), 5.81 (t, 1H, $J_{2,3} = J_{3,4}$ = 9.7 Hz, H-3), 5.51 (d, 1H, $J_{1,2}$ = 10.6 Hz, H-1), 5.02 (t, 1H, $J_{3,4} = J_{4,5}$ = 9.7 Hz, H-4), 4.62 (t, 1H, H-2), 4.13 and 4.21 (AB part of ABX pattern, 2H, $J_{6a,6b}$ = 12.8 Hz, $J_{5,6a} = J_{5,6b}$ = 4.8 Hz, 2 H-6), 3.88 (m, 1H, H-5), 2.01, 2.00, 1.99 (3s, 9H, 3 Ac). ^{13}C NMR (100 MHz) δ: 170.0, 169.8, 168.9 (3 Ac C=O), 167.9 (2 phth C=O), 137.9, 130.1, 128.6, 123.4 (S-Ph C), 134.2, 131.3, 124.4 (Phth C), 86.1 (C-1), 76.3 (C-5), 71.2 (C-3), 67.8 (C-4), 61.4 (C-6), 49.4 (C-2), 20.3, 20.2, 20.0 (Ac Me).

This compound decomposed on standing into a compound (R_f = 0.82, 5% acetone in chloroform) that was purified by flash chromatography on silica gel (3% acetone in dichloromethane) as a syrup, identified as 3,4,6-tri-*O*-acetyl-2-deoxy-2-phthalimido-D-glucal; $[\alpha]_D^{25}$ – 15.7° (*c* 5.1, chloroform), lit.[67] $[\alpha]_D$ – 15.0°. ^{1}H NMR (250.13 MHz) δ: 7.96–7.74 (AA′BB′ pattern, 4H, Phth-H), 6.78 (s, 1H, H-1), 5.61 (d, 1H, $J_{3,4}$ = 4.0 Hz, H-1), 5.33 (t, 1H, $J_{4,5}$ = 4.4 Hz, H-4), 4.54 (m, 2H, H-5, H-6a), 4.40 (m, 1H, H-6b), 2.16, 2.14, 1.94 (3s, 9H, 3 Ac). ^{13}C NMR (100 MHz) δ: 170.1, 169.9, 168.9 (3 Ac C=O), 167.9 (2 phth C=O), 148.2 (C-1), 134.3, 131.6, 123.7 (Phth C), 105.6 (C-2), 74.6 (C-5), 67.3 (C-3), 65.7 (C-4), 61.1 (C-6), 20.8, 20.6, 20.2 (Ac Me). HR-MS (EI) *m*/*z* calcd. for $C_{20}H_{19}NO_9$: 417.1059; found: 417.1045.

Supplementary data

Supplementary data for this article are available on the journal Web site (canjchem.nrc.ca). CCDC 782358–782362 contain the X-ray data in CIF format for this manuscript. These data can be obtained, free of charge, via www.ccdc.cam.ac.uk/conts/retrieving.html (or from the Cambridge Crystallographic Data Centre, 12 Union Road, Cambridge CB2 1EZ, UK; fax +44 1223 336033; or deposit@ccdc.cam.ac.uk).

Supplementary data for this article are available on the journal Web site (canjchem.nrc.ca).

Acknowledgements

We thank the Natural Sciences and Engineering Research Council of Canada (NSERC) for financial support and the Atlantic Region Magnetic Resonance Centre (ARMRC) for NMR time. We thank Dr. B.M. Pinto for discussions and a referee for a suggestion. Some of the computational facilities were provided by the Atlantic Computational Excellence network (ACEnet), the regional high-performance computing consortium for universities in Atlantic Canada. ACEnet is funded by the Canada Foundation for Innovation (CFI), the Atlantic Canada Opportunities Agency (ACOA), and the provinces of Newfoundland and Labrador, Nova Scotia, and New Brunswick.

References

(1) Kahne, D.; Walker, S.; Cheng, Y.; van Engen, D. *J. Am. Chem. Soc.* **1989**, *111* (17), 6881. doi:10.1021/ja00199a081.
(2) Aversa, M. C.; Barattucci, A.; Bonaccorsi, P. *Tetrahedron* **2008**, *64* (33), 7659. doi:10.1016/j.tet.2008.05.051.
(3) Yan, L.; Kahne, D. *J. Am. Chem. Soc.* **1996**, *118* (39), 9239. doi:10.1021/ja9608555.
(4) Nicolaou, K. C.; Mitchell, H. J.; Rodriguez, R. M.; Fylaktakidou, K. C.; Suzuki, H.; Conley, S. R. *Chem. Eur. J.* **2000**, *6* (17), 3149. doi:10.1002/1521-3765(20000901)6:17<3149::AID-CHEM3149>3.0.CO;2-L.
(5) Crich, D.; Dai, Z. M. *Tetrahedron* **1999**, *55* (6), 1569. doi:10.1016/S0040-4020(98)01202-2.
(6) Gadikota, R. R.; Callam, C. S.; Wagner, T.; Del Fraino, B.; Lowary, T. L. *J. Am. Chem. Soc.* **2003**, *125* (14), 4155. doi:10.1021/ja029302m. PMID:12670238.
(7) Houseknecht, J. B.; Lowary, T. L. *J. Org. Chem.* **2002**, *67* (12), 4150. doi:10.1021/jo011127p. PMID:12054950.
(8) Dudkin, V. Y.; Miller, J. S.; Danishefsky, S. J. *Tetrahedron Lett.* **2003**, *44* (9), 1791. doi:10.1016/S0040-4039(03)00101-1.
(9) Zhang, H.; Wang, Y. L.; Thurmer, R.; Meisenbach, M.; Voelter, W. *Liebigs Ann./Recl.* **1997**, 1871. doi:10.1002/jlac.199719970910.
(10) Wipf, P.; Reeves, J. T. *J. Org. Chem.* **2001**, *66* (23), 7910. doi:10.1021/jo015952h. PMID:11701059.
(11) Crich, D.; Banerjee, A.; Yao, Q. J. *J. Am. Chem. Soc.* **2004**, *126* (45), 14930. doi:10.1021/ja047194t. PMID:15535720.
(12) Crich, D.; Pedersen, C. M.; Bowers, A. A.; Wink, D. J. *J. Org. Chem.* **2007**, *72* (5), 1553. doi:10.1021/jo061440x. PMID:17286432.
(13) Taylor, J. G.; Li, X. C.; Oberthür, M.; Zhu, W. J.; Kahne, D. E. *J. Am. Chem. Soc.* **2006**, *128* (47), 15084. doi:10.1021/ja065907x. PMID:17117848.
(14) Bai, Y.; Lowary, T. L. *J. Org. Chem.* **2006**, *71* (26), 9658. doi:10.1021/jo061713o. PMID:17168583.
(15) Yan, L.; Taylor, C. M.; Goodnow, R., Jr.; Kahne, D. *J. Am. Chem. Soc.* **1994**, *116* (15), 6953. doi:10.1021/ja00094a067.
(16) Ferrières, V.; Joutel, J.; Boulch, R.; Roussel, M.; Toupet, L.; Plusquellec, D. *Tetrahedron Lett.* **2000**, *41* (29), 5515. doi:10.1016/S0040-4039(00)00887-X.
(17) Khiar, N.; Fernández, I.; Araújo, C. S.; Rodríguez, J.-A.; Suárez, B.; Álvarez, E. *J. Org. Chem.* **2003**, *68* (4), 1433. doi:10.1021/jo026519q. PMID:12585884.

(18) Safatli, M. *MSc. Thesis;* Dalhousie University: Halifax, NS, 1998.
(19) Lemieux, R. U.; Koto, S.; Voisin, D. The Exoanomeric Effect. In *Anomeric Effect: Origin and Consequences;* Szarek, W. A., Horton, D., Eds.; American Chemical Society: Washington, DC, 1979; p 17.
(20) Kirby, A. J. *The Anomeric Effect and Related Stereoelectronic Effects at Oxygen;* Springer-Verlag: New York, 1983.
(21) Tvaroška, I.; Bleha, T. *Adv. Carbohydr. Chem. Biochem.* **1989**, *47*, 45. doi:10.1016/S0065-2318(08)60412-6.
(22) Juaristi, E.; Cuevas, G. *The Anomeric Effect;* CRC Press: Boca Raton, FL, 1994.
(23) Crich, D.; Mataka, J.; Zakharov, L. N.; Rheingold, A. L.; Wink, D. J. *J. Am. Chem. Soc.* **2002**, *124* (21), 6028. doi:10.1021/ja0122694. PMID:12022836.
(24) Cramer, C. J.; Truhlar, D. G.; French, A. D. *Carbohydr. Res.* **1997**, *298* (1–2), 1. doi:10.1016/S0008-6215(96)00297-2.
(25) Tvaroška, I.; Carver, J. P. *Carbohydr. Res.* **1998**, *309* (1), 1. doi:10.1016/S0008-6215(98)00114-1.
(26) Khiar, N. *Tetrahedron Lett.* **2000**, *41* (47), 9059. doi:10.1016/S0040-4039(00)01651-8.
(27) Houk, K. N.; Eksterowicz, J. E.; Wu, Y.-D.; Fuglesang, C. D.; Mitchell, D. B. *J. Am. Chem. Soc.* **1993**, *115* (10), 4170. doi:10.1021/ja00063a040.
(28) Crich, D.; Mataka, J.; Sun, S.; Wink, D. J.; Lam, K.-C.; Rheingold, A. L.; Wink, D. *J. Chem. Commun. (Camb.)* **1998**, 2763. doi:10.1039/a804126a.
(29) Crich, D.; Sun, S. X. *Tetrahedron* **1998**, *54* (29), 8321. doi:10.1016/S0040-4020(98)00426-8.
(30) Crich, D.; Cai, W. L.; Dai, Z. M. J. *Org. Chem.* **2000**, *65* (5), 1291. doi:10.1021/jo9910482.
(31) Misbahi, K.; Lardic, M.; Ferrières, V.; Noiret, N.; Kerbal, A.; Plusquellec, D. *Tetrahedron: Asymmetry* **2001**, *12* (17), 2389. doi:10.1016/S0957-4166(01)00437-2.
(32) Khiar, N.; Alonso, I.; Rodriguez, N.; Fernandez-Mayoralas, A.; Jimenez-Barbero, J.; Nieto, O.; Cano, F.; Foces-Foces, C.; Martin-Lomas, M. *Tetrahedron Lett.* **1997**, *38* (47), 8267. doi:10.1016/S0040-4039(97)10164-2.
(33) Buist, P. H.; Behrouzian, B.; MacIsaac, K. D.; Cassel, S.; Rollin, P.; Imberty, A.; Gautier, C.; Pérez, S.; Genix, P. *Tetrahedron: Asymmetry* **1999**, *10* (15), 2881. doi:10.1016/S0957-4166(99)00294-3.
(34) Aversa, M. C.; Barattucci, A.; Bonaccorsi, P.; Bruno, G.; Giannetto, P.; Rollin, P. *Lett. Org. Chem.* **2004**, *1* (4), 376. doi:10.2174/1570178043400631.
(35) Buist, P. H.; Behrouzian, B.; Cassel, S.; Lorin, C.; Rollin, P.; Imberty, A.; Pérez, S. *Tetrahedron: Asymmetry* **1997**, *8* (12), 1959. doi:10.1016/S0957-4166(97)00207-3.
(36) Miyajima, K.; Nekado, T.; Ikeda, K.; Achiwa, K. *Chem. Pharm. Bull. (Tokyo)* **1998**, *46* (11), 1676. PMID:9845951.
(37) Lemieux, R. U.; Ratcliffe, R. M. *Can. J. Chem.* **1979**, *57* (10), 1244. doi:10.1139/v79-203.
(38) Cheshev, P. E.; Kononov, L. O.; Tsvetkov, Y. E.; Shashkov, A. S.; Nifantiev, N. E. *Russ. J. Bioorganic Chem.* **2002**, *28* (5), 419. doi:10.1023/A:1020428329743.
(39) Crich, D.; Cai, W. L. *J. Org. Chem.* **1999**, *64* (13), 4926. doi:10.1021/jo990243d. PMID:11674572.
(40) Spek, A. L. *PLATON;* a multipurpose crystallographic tool; Utrecht University: Utrecht, The Netherlands, 2003.
(41) Wolinski, K.; Hinton, J. F.; Pulay, P. *J. Am. Chem. Soc.* **1990**, *112* (23), 8251. doi:10.1021/ja00179a005.
(42) Forsyth, D. A.; Sebag, A. B. *J. Am. Chem. Soc.* **1997**, *119* (40), 9483. doi:10.1021/ja970112z.
(43) Stott, K.; Stonehouse, J.; Keeler, J.; Hwang, T. L.; Shaka, A. J. *J. Am. Chem. Soc.* **1995**, *117* (14), 4199. doi:10.1021/ja00119a048.
(44) Neuhaus, D.; Williamson, M. P. *The Nuclear Overhauser Effect in Structural and Conformational Analysis;* Wiley-VCH, Inc.: New York, 2000.
(45) Lemieux, R. U.; Takeda, T.; Chung, B. Y. Synthesis of 2-Amino-2-deoxy-β-D-glucopyranosides. In *Synthetic Methods for Carbohydrates;* El Khadem, H. S., Ed.; American Chemical Society: Washington, DC, 1976; p 90.
(46) Dasgupta, F.; Garegg, P. J. J. *Carbohydr. Chem.* **1988**, *7* (3), 701. doi:10.1080/07328308808057560.
(47) Medgyes, A.; Farkas, E.; Lipták, A.; Pozsgay, V. *Tetrahedron* **1997**, *53* (12), 4159. doi:10.1016/S0040-4020(97)00145-2.
(48) Jain, R. K.; Matta, K. L. *Carbohydr. Res.* **1992**, *226* (1), 91. doi:10.1016/0008-6215(92)84057-Y. PMID:1499025.
(49) Cuesta, I. G.; De Merás, A. S.; Pelloni, S.; Lazzeretti, P. *J. Comput. Chem.* **2009**, *30* (4), 551. doi:10.1002/jcc.21083. PMID:18711723.
(50) Lazzeretti, P. *Prog. Nucl. Magn. Reson. Spectrosc.* **2000**, *36* (1), 1. doi:10.1016/S0079-6565(99)00021-7.
(51) Duddeck, H.; Korek, U.; Rosenbaum, D.; Drabowicz, J. *Magn. Reson. Chem.* **1986**, *24* (9), 792. doi:10.1002/mrc.1260240911.
(52) Frisch, M. J.; Trucks, G. W.; Schlegel, H. B.; Scuseria, G. E.; Robb, M. A.; Cheeseman, J. R.; Montgomery, J. A., Jr.; Vreven, T.; Kudin, K. N.; Burant, J. C.; Millam, J. M.; Iyengar, S. S.; Tomasi, J.; Barnone, V.; Mennucci, B.; Cossi, M.; Scalmani, G.; Nega, N.; Petersson, G. A.; Nakatsuji, H.; Haha, M.; Ehara, M.; Toyota, K.; Fukuda, R.; Hasegawa, J.; Ishida, M.; Nakajima, T.; Honda, Y.; Kitao, O.; Nakai, H.; Klene, M.; Li, X.; Knox, J. E.; Hratchian, H. P.; Cross, J. B.; Adamo, C.; Jaramillo, J.; Gomperts, R.; Stratmann, R. E.; Yazyev, O.; Austin, J.; Cammi, R.; Pomelli, C.; Ochterski, J. W.; Ayala, P. Y.; Morokuma, K.; Voth, G. A.; Salvador, P.; Dannenberg, J. J.; Zakrzewski, V. G.; Dapprich, S.; Daniels, A. D.; Strain, M. C.; Farkas, O.; Malick, D. K.; Rabuck, A. D.; Raghavachari, K.; Foresman, J. B.; Ortiz, J. V.; Cui, Q.; Baboul, A. G.; Clifford, S.; Cioslowski, J.; Stefanov, B. B.; Liu, G.; Liashenko, A.; Piskorz, P.; Peng, C. Y.; Nanayakkara, A.; Challacombe, M.; Gill, P. M. W.; Johnson, B.; Chen, W.; Wong, M. W.; Gonzales, C.; Pople, J. A. *Gaussian 03;* Gaussian, Inc.: Wallingford, CT, 2003.
(53) Becke, A. D. *J. Chem. Phys.* **1993**, *98* (7), 5648. doi:10.1063/1.464913.
(54) Becke, A. D. *J. Chem. Phys.* **1993**, *98* (2), 1372. doi:10.1063/1.464304.
(55) Sinnokrot, M. O.; Valeev, E. F.; Sherrill, C. D. *J. Am. Chem. Soc.* **2002**, *124* (36), 10887. doi:10.1021/ja025896h. PMID:12207544.
(56) Tvaroška, I.; Bleha, T. *Can. J. Chem.* **1979**, *57* (4), 424. doi:10.1139/v79-069.
(57) Watts, J.; Jiménez-Barbero, J.; Poveda, A.; Grindley, T. B. *Can. J. Chem.* **2003**, *81* (5), 364. doi:10.1139/v03-062.
(58) Hunter, C. A.; Sanders, J. K. M. *J. Am. Chem. Soc.* **1990**, *112* (14), 5525. doi:10.1021/ja00170a016.
(59) Grover, J. R.; Walters, E. A.; Hui, E. T. *J. Phys. Chem.* **1987**, *91* (12), 3233. doi:10.1021/j100296a026.
(60) Sinnokrot, M. O.; Sherrill, C. D. *J. Am. Chem. Soc.* **2004**, *126* (24), 7690. doi:10.1021/ja049434a. PMID:15198617.
(61) Krause, H.; Ernstberger, B.; Neusser, H. *J. Chem. Phys. Lett.* **1991**, *184* (5–6), 411. doi:10.1016/0009-2614(91)80010-U.
(62) North, A. C. T.; Phillips, D. C.; Mathews, F. S. *Acta Crystallogr.* **1968**, *A24*, 351.

(63) Molecular Structure Corporation. *TEXSAN for Windows,* version 1.06; single crystal structure analysis software; Molecular Structure Corporation: The Woodlands, TX, 1999.
(64) Altomare, A.; Cascarano, M.; Giacovazzo, C.; Guagliardi, A.; Burla, M. C.; Polidori, G.; Camalli, M. *J. Appl. Cryst.* **1994**, *27* (3), 435. doi:10.1107ÕS002188989400021X.
(65) Altomare, A.; Cascarano, G.; Giacovazzo, C.; Guagliardi, A. *J. Appl. Cryst.* **1993**, *26* (3), 343. doi:10.1107/S0021889892010331.
(66) Sheldrick, G. M. *SHELXL-97,* release 97-2; programs for crystal structure analysis; Institute für Anorganische Chemie, Universität Göttingen, Germany, 1998.
(67) Ogawa, T.; Nakabayashi, S.; Sasajima, K. *Carbohydr. Res.* **1981**, *95* (2), 308. doi:10.1016/S0008-6215(00)85587-1.